Brain Structure and Function (2020) 225:763–784
https://doi.org/10.1007/s00429-020-02034-5

ORIGINAL ARTICLE

The role of the posterior parietal cortex in saccadic error processing

Jérôme Munuera[1,2,3] · Jean-René Duhamel[1]

Received: 23 April 2019 / Accepted: 27 January 2020 / Published online: 17 February 2020

Abstract

Ocular saccades rapidly displace the fovea from one point of interest to another, thus minimizing the loss of visual information and ensuring the seamless continuity of visual perception. However, because of intrinsic variability in sensory-motor processing, saccades often miss their intended target, necessitating a secondary corrective saccade. Behavioral evidence suggests that the oculomotor system estimates saccadic error by relying on two sources of information: the retinal feedback obtained post-saccadically and an internal extra-retinal signal obtained from efference copy or proprioception. However, the neurophysiological mechanisms underlying this process remain elusive. We trained two rhesus monkeys to perform visually guided saccades towards a target that was imperceptibly displaced at saccade onset on some trials. We recorded activity from neurons in the lateral intraparietal area (LIP), an area implicated in visual, attentional and saccadic processing. We found that a subpopulation of neurons detect saccadic motor error by firing more strongly after an inaccurate saccade. This signal did not depend on retinal feedback or on the execution of a secondary corrective saccade. Moreover, inactivating LIP led to a large and selective increase in the latency of small (i.e., natural) corrective saccade initiation. Our results indicate a key role for LIP in saccadic error processing.

Keywords Parietal cortex · Oculomotor control · Non-human primate · Neurophysiology · Muscimol

Introduction

When exploring a visual scene, we make frequent saccades to direct the fovea from one point of interest to another. Despite its remarkable performance, the saccadic system can be inaccurate because of intrinsic sensorimotor variability (van Beers et al. 2004; van Beers 2007, 2008). When a primary saccade (PS) undershoots or overshoots a visual target, a secondary corrective saccade (CS) is sometimes generated to align the fovea on the target (Becker 1991). Saccadic error estimation rests on post-saccadic retinal and extra-retinal (proprioceptive feedback and/or efference copy of the motor command) cues which are optimally weighted to achieve post-saccadic error correction (Munuera et al. 2009; Morel et al. 2011; Joiner et al. 2010, 2013). Saccadic error processing also plays an important role in saccadic adaptation (Wong and Shelhamer 2012) for re-calibrating oculomotor commands (Shadmehr et al. 2010). The likelihood of a CS increases with PS inaccuracy as expected (Deubel et al. 1982; Becker 1991), although evidence suggests that errors below and above 3° of amplitude are processed differently. First, for large visually guided saccades (20°–40°) that usually generate errors of about 2°–4° in amplitude, the latency of CS decreases with increasing error size but asymptotes at around 3° (Becker 1991). This 3° limit corresponds to the cone photoreceptor-rich fovea where visual acuity is maximal and which is crucial for reading and object details recognition (Daniel and Whitteridge 1961; Rayner 1998). Contrary to small errors that are sometimes tolerated (because target visibility after the PS is sufficient for most perceptual needs), errors larger than 3°–4° are systematically corrected, even in total darkness when the target is turned off during the primary saccade, suggesting that large CS can be triggered

✉ Jérôme Munuera
jerome.munuera@icm-institute.org

✉ Jean-René Duhamel
duhamel@isc.cnrs.fr

[1] Institut Des Sciences Cognitives Marc Jeannerod, Centre National de La Recherche Scientifique, UMR 5229, Bron, France

[2] Institut du Cerveau et de la Moelle épinière, ICM, Inserm U 1127, CNRS UMR 7225, Sorbonne Université, F-75013 Paris, France

[3] Institut Jean Nicod, Département d'études cognitives, ENS, EHESS, CNRS, PSL University, 75005 Paris, France

by an extra-retinal feedback mechanism (Weber and Daroff 1972; Prablanc and Jeannerod 1975; Becker 1991).

Despite several studies, the neural mechanisms and structures involved in saccadic error processing remain poorly understood and somewhat controversial. It has been suggested that the superior colliculus (SC) is involved in oculomotor error processing (Waitzman et al. 1988) but later experiments postulated that this area is primarily involved in the encoding of the distance to the visual target and not saccade amplitude (Bergeron et al. 2003). The role of the cerebellum is also often emphasized (Goffart et al. 2004; Panouillères et al. 2013), though the exact contribution of different cell types are still debated (Robinson and Fuchs 2001; Thier et al. 2002; Soetedjo and Fuchs 2006; Popa et al. 2016). Whether saccadic error is processed by other brain areas, like the frontal eye field (FEF) or the lateral intraparietal area (LIP) remains an open question. Area LIP has been implicated in visual, attentional, oculomotor and information expectancy mechanisms (Gnadt and Andersen 1988; Andersen et al. 1992; Colby et al. 1996; Gottlieb et al. 1998; Horan et al. 2019) and provides a nice window into studying decision-making processes (Huk et al. 2017). Prior studies have shown that LIP updates its representation of visual stimuli in conjunction with saccades (Duhamel et al. 1992), most likely via an efference copy mechanism (Sommer and Wurtz 2002, 2006; 2008). Since LIP neurons respond to visual targets, before, during and/or after saccades (Barash et al. 1991a, b), this area contains, in principle, many elements required for saccadic error computation. One study recently described a class of LIP neurons that respond vigorously to the appearance of a visual target before saccade execution, and later on, after the end of the saccade, with low-rate activity that was correlated with saccadic error and corrective saccade probability (Zhou et al. 2016). Given that these neurons carry different information and that the observed error signal arises relatively late, i.e., 150–350 ms after the end of the primary saccade, it is unclear whether such activity reflects error coding, visual feedback or motor preparation and whether this implies a functional role of LIP in saccade correction. Here, we analyze the role of LIP in saccade error processing, focusing on a different subset of LIP neurons that exhibited "pure" post-saccadic activity and we test the implication of LIP in corrective mechanisms by means of reversible inactivation. Early work aimed at characterizing saccade-related neuronal activity in posterior parietal cortex indicated that a main distinguishing feature between area LIP and neighboring area 7a on the cortical convexity is that the latter region tends to discharge later and shows more post-saccadic activity than LIP (Barash et al. 1991a, b). However, post-saccadic neurons are present in both areas, and the study by Zhou et al. (2016) established the presence within LIP of post-saccadic neurons intermingled with other cell types such as "classical" LIP visuo-motor neurons. The role of LIP post-saccadic neurons is unclear. To test the hypothesis that such neurons carry a selective saccadic error signal, i.e., that they detect the discrepancy between the programmed and executed saccade, we recorded from area LIP in two monkeys performing visually guided saccades towards a peripheral target. On some trials, this target was imperceptibly displaced at saccade onset to dissociate retinal and extra-retinal sources of error feedback. In other words, we considered saccades as accurate or inaccurate with respect to the original saccadic target position, i.e., the position of the target ahead of its displacement at saccade onset, and independently of the size and direction of the displacement. LIP post-saccadic neurons showed enhanced activity after inaccurate saccades compared to accurate ones. This neural modulation was triggered by extra-retinal information about saccadic error. We then inactivated LIP unilaterally and found a selective increase in the latency of small CSs (i.e., equivalent in size to the range of natural variability of the saccadic system) following inaccurate contraversive PSs. This result indicates a functional role for LIP in saccadic error processing as postulated by our neural recordings (error detection) and by previous results (error correction) (Zhou et al. 2016).

Materials and methods

Animal preparation

The present experiment follows procedures in compliance with European Communities Council Directive of 2010 (2010/63/UE) as well as the recommendations of the French National Ethics Committee. Two adult female rhesus monkeys (*Macaca mulatta*) weighing 4.5 kg and 6 kg (monkey N and monkey S) underwent a single surgical session to prepare for chronic recording of eye movements and extracellular recording within the parietal cortex. Anesthesia was induced with tiletamine/zolazepam (15 mg/kg) and maintained under isoflurane (2.5%). Animals were given atropine (0.25 mg/kg) to prevent excessive salivation. Adequate measures were taken to minimize pain or discomfort during and after surgery. Analgesia was provided by a presurgical buprenorphine injection (0.2 mg/kg). The animals were implanted with scleral search coils (Judge et al. 1980), head-restraining posts and recording chambers (Crist Instruments, Damascus, MD). The chambers were positioned over craniotomies performed in the right and left hemisphere for monkey N and monkey S, respectively, at stereotaxic LIP coordinates (P5, L12). To facilitate the introduction of recording microelectrodes, the dural surface was kept thin thanks to periodic removal of granulation tissue under light anesthesia (tiletamine/zolazepam, 15 mg/kg and local irrigation with lidocaine spray). Monkeys were euthanized and perfused at

the end of the experiments. Their brains were processed for histological verification of electrode and injection cannula sites (Fig. 1a).

Experimental design

The experimental sessions were conducted in a darkened room. Throughout the session, the monkeys were seated in a primate chair with their head restrained. They faced a tangent translucent screen 57 cm away, which spanned 120° × 90° of the visual field. We used a video projector (Optoma EzPro737) at 60 Hz refresh rate, which back-projected the stimuli on the screen. Horizontal and vertical eye movements were recorded continuously with the magnetic search coil technique (Primelec, Regensdorf, Switzerland) and digitized and stored at 250 Hz. Behavioral paradigms, storage of both neuronal discharges and eye movements, and real-time saccade detection were performed using the REX software (Hays et al. 1982) running on the real-time QNX operating system. Visual stimuli were generated on a slave computer running our own software (Spartacus) with a frame rate of 60 Hz. This experimental control system allowed modifying the visual display contingent upon detection of saccade onset (using a velocity threshold set at) with an average delay of 30 ms. Synchronization of visual stimuli with eye movement and neural recordings was checked

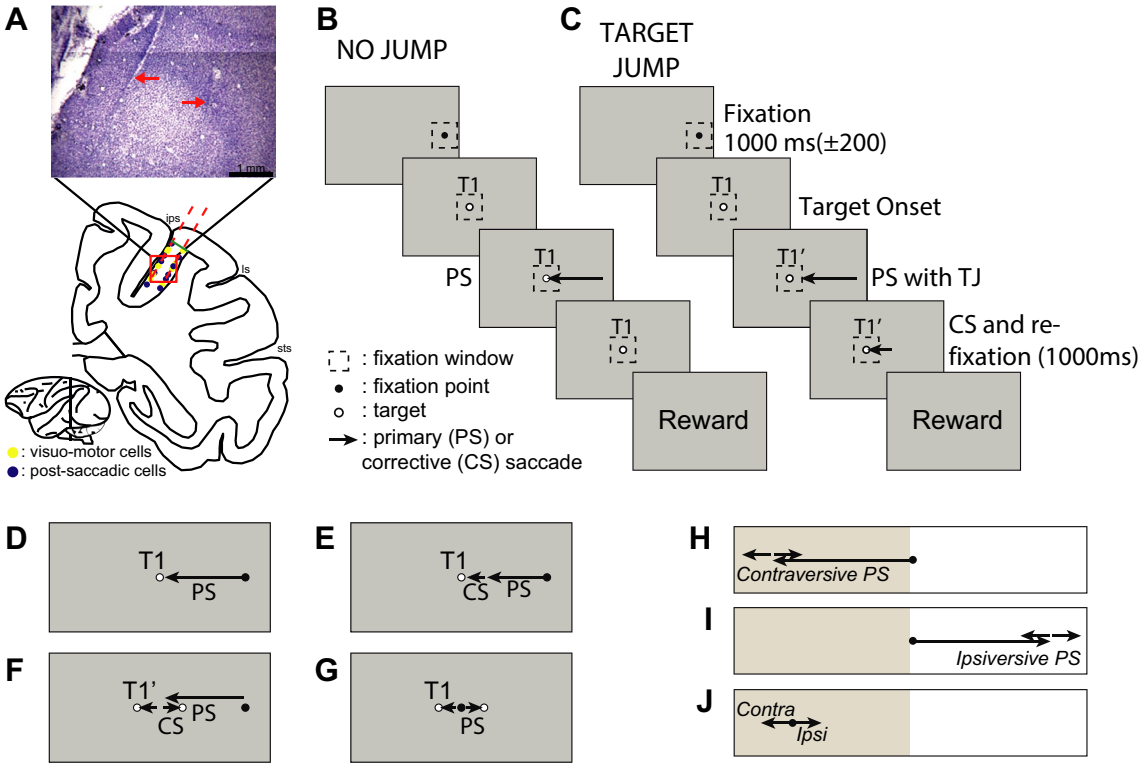

Fig. 1 Description of the experiments. **a** Histological reconstruction of two representative recording/inactivation sites in LIP (monkey N). Red arrows on the photomicrograph represent the track of the electrodes and/or cannulas. Yellow and blue dots on the drawing of the coronal section represent, respectively, the location of the visuo-motor and post-saccadic neurons along the tracks based on logs of recording depth. The green line marks the limit between LIP and area 7a. **b** No-jump trials consisted of the basic visually guided saccadic task where monkeys had to re-foveate a visual target (T1) with a saccadic eye movement after a fixation point disappearance/target onset to successfully complete the trial. **c** In the target-jump (TJ) trials, the visual target was displaced during the execution of the primary saccade (PS) which induced a corrective saccade (CS) to adjust the fovea on the new target position (T1′). Note that CS could be consecutive to a target jump in target-jump condition but also to an inaccurate PS (target-jump and no-jump trials). **d**–**g** Representation of the main saccade conditions used in the single-neuron recording experiment. All these trial types were randomly interleaved. **d** In no-jump condition, T1 was in the response field of the recorded neuron. **e** When PS was inaccurate, a CS was executed to ensure that the eye was in the fixation window. **f** In target-jump trials during the PS, an intra-saccadic target jump unpredictably occurred in the same or different direction as the PS, producing a CS to T1′. **g** In small PS trials T1 appeared at each possible T1′ position encountered in the target-jump trials. **h**–**j** Schematic representation of the target positions in the inactivation experiment. **h** Eye started from the fixation point at the center of the screen towards a peripheral target. During the PS in the visual field contralateral to the injection sites (brown-shaded area: inactivated field), the target remained stable (no-jump) or was unpredictably displaced to a new position backwards or forwards from the initial target position (target jump) like in the single-neuron recording experiment. This target jump also induced, in most cases, a CS towards the new target position (small arrows). CS can also be observed in no-jump trials. **i** The same type of trials was also performed in the field ipsilesional to the inactivated field. **j** Representation of the small PS trials performed in the contralesional field

offline using records of TTL signals emitted by a photoprobe positioned at the border of the screen where a one-frame light pulse was emitted at each stimulus transition (onset and offset). This pulse was not visible to the monkey.

Neurophysiological recordings

Activity of well-isolated single neurons was recorded extracellularly in the lateral bank of the intraparietal sulcus using tungsten microelectrodes (Frederick Haer, Bowdoin, ME; 1–2 MΩ at 1 kHz), which were lowered by means of a hydraulic microdrive (Narishige, Tokyo, Japan) through a stainless steel guide tube that rested on but did not perforate the dura and overlying granulation tissue. The guide tube was held in place thanks to a grid with grid holes covering the entire recording chamber. Extracellular activities were amplified using a Neurolog system (Digitimer, Hertfordshire, UK) and were digitized with MSD (Alpha-Omega, Nazareth, Israel) hardware and software to discriminate the spikes and neuron selectivity online. We identified LIP using standard criteria to distinguish it from adjacent IPS areas (Gnadt and Andersen 1988; Colby et al. 1996), using various visual stimulation and eye movement tasks (see below). Electrode penetrations were made perpendicular to the cortical surface and into the lateral bank of the intraparietal sulcus. The LIP recordings sites were located between 3 and 8 mm (mm) below the cortical surface, which was identified by the sharp transition between absence and presence of neural signal as the electrode was advanced through the meninges and entered the brain. Single-unit responses were characterized by manual testing of receptive field properties and with standard oculomotor tasks (overlap saccades). The ventral border of LIP was easily identified by the transition between responses to stationary visual stimuli and to saccades and responses to moving stimuli and to tactile stimulation of the face typical of the ventral intraparietal (VIP) area. The dorsal LIP/7a border is more difficult to identify using neuronal response properties, but since most of the neurons were recorded below a depth of 3 mm, we considered them to be located mainly in area LIP. Within these dorsal and ventral physiological borders, we considered neurons to be in LIP if they showed consistent visual and/or saccade-associated response during the overlap saccade task or were located between such neurons in that electrode penetration. Recording and microinjection sites could be verified histologically in one animal (Fig. 1a).

In the foregoing description of experimental procedures, we use the terms "contra" and "ipsi" to refer to an eye movement direction or a visual hemifield location with regard to the recorded/injected hemisphere. Hence, the terms "contraversive" and "ipsiversive" refer to saccades directed, respectively, away from and towards the recorded/inactivated hemisphere, and the terms "contralesional" and "ipsilesional" refer to the visual hemifield located, respectively, opposite to or on the same side as the inactivated hemisphere.

Inactivation

Four inactivation and five control sessions were conducted in alternation in each monkey. To inactivate LIP, we administered muscimol, a GABAA agonist following a previously employed procedure in our lab (Wardak et al. 2002, 2004). Muscimol was concentrated at 5 µg/µl in physiological saline. The solution was injected through a stainless steel needle (29 gauge) connected to a 5 µl Hamilton syringe. We used the same grid and the Narishige microdrive for the electrophysiological and inactivation experiments. Each inactivation session involved injections at four sites (two rostro-caudal locations and two depths within the lateral bank of the intraparietal sulcus). These sites and their associated grid holes were selected based on the visual and saccadic neural responses recorded during prior electrophysiological experiments (i.e., the same sites as in our single-neuron recordings with clear and consistent LIP visuo-saccadic and post-saccadic responses). Two needles were inserted in parallel through the grid holes into the cortex. To maximize the inactivation effects, injections were performed in rapid successions at two different depths (bottom sites at 6 mm and top sites at 4 mm from the surface of the cortex) in each needle track, separated by 3 mm, for a total of four points of injections, thus inactivating a large portion of LIP, including its dorsal and ventral parts (Liu et al. 2010). At each injection point, 1.5 (bottom sites) or 1 µl (top sites) of solution was injected. To avoid tissue pressure, injections were performed manually by steps of 0.5 µl, 1 min apart. The interval between injections at the two depths within a track was approximately 10 min. The two needles were left in place after the last injections and removed only at the end of the experiment. The onset of muscimol effects was assessed using a saccadic choice task that the monkeys started to perform 5 min after the last injection and unfolded as follows: when monkeys fixated a central fixation spot, two visual targets appeared on the horizontal meridian at 20° eccentricity in the ipsilesional and contralesional hemifields and monkeys were rewarded for making a saccade to either target. Visual targets of the main task were also presented along the horizontal meridian. The presence of a clear ipsilesional bias ($\geq$ 80% for a block of 25 trials) in target selection (relative to pre-injection and to control sessions where the choice probability was ~ 50%) was considered, in close line with previous studies (Wardak et al. 2002, 2004), as an indicator of LIP inactivation, at least within the region of visual field where the targets of the main task will be presented. We then started the behavioral acquisition on the main task ~ 15 min after this bias towards the ipsilesional targets manifested. The effects of muscimol started 20–50 min post-injection

and were still present after the data acquisition (validated with the saccadic choice task showing the persistence of the choice bias).

Two of the five control sessions involved physiological saline injection using the same injection procedures and locations as the muscimol injections to check for possible effects on behavioral performance of the presence of the needles and liquid pressure in the tissue. Since we did not find any difference between NaCl and no-injection sessions, data from the five control experiments were pooled for statistical analyses.

Functional characterization of LIP neurons

During the single-neuron recording sessions, we characterized manually each neuron's spatial tuning to visual stimuli and saccades by having the monkey perform a standard visually guided saccade task. Using a joystick interface, the experimenter could select a new target position on every trial and thereby sample the monkey's entire visual field while visualizing online the neuronal response, until the center of the cell's response field, i.e., its preferred visual target position and/or saccade direction and amplitude (e.g., perifoveal vs. peripheral) was identified. We monitored neural activity during standard overlap saccadic task (see below) to this preferred target to check for distinct visual and saccadic response components. We used this response profile as online criterion that our electrode was located in area LIP. Finally, we recorded and stored the activity of all neurons during the overlap saccade task, which unfolded as follows: after the monkey foveated a fixation point ($0.1° \times 0.1°$) at the center of the screen, a peripheral visual target was turned on at the center of the cell's response field and remained on for 600–800 ms (ms); following this delay, the fixation point was extinguished, cueing the monkey to execute the saccade to the target. Data from this task served in offline analyses to document LIP neurons' visual and saccade-related properties and identify post-saccadic neurons.

Main experimental task

Following this initial characterization, each cell was tested using an intra-saccadic target-jump task. The target-jump protocol was similar in design to previous studies investigating saccadic error processing in both psychophysical (Deubel et al. 1982; Munuera et al. 2009) and single-neuron recording experiments (Soetedjo et al. 2008a, b) and consisted of a modified standard visually guided saccade task with three different trial conditions: a no-jump condition, a target-jump condition (TJ), and a small primary saccade condition (small PS). Behaviorally, the monkeys had to perform at least 15 correct trials for the different trial types described below.

No-jump trials

Monkeys were required to foveate a fixation point (FP, $0.1° \times 0.1°$). The fixation point was extinguished after 1000 ms (±200 ms range). Simultaneously to fixation point offset, a peripheral target (T1, size $0.1° \times 0.1°$) was turned on. The monkeys had to execute a saccade to T1 within 500 ms after T1 onset and maintain fixation within a tolerance window centered on T1 for 1000 ms to obtain a drop of juice reward (Fig. 1b). This differs from the overlap control task where the monkeys had to maintain fixation for 600 ms with the target already on the screen. The size of this window was compatible with the natural variation of PS accuracy (see below). Thus, even though the fovea was not perfectly on the target, the monkey could receive the reward. In the single-neuron recording experiment, the fixation point was placed at a peripheral location and T1 at the center of the screen, such that T1 fell at the center of the cell's previously defined response field (RF) (mean ~ 20° ± 15° range in the contralateral field, across the recorded neuronal population, Fig. 1d, e). In the inactivation experiment, the fixation point appeared at the center of the screen and T1 was always presented at 15° or 30° of eccentricity on the horizontal meridian in the right or left hemifield (Fig. 1h, i): in monkey N, the right hemifield was contralesional, while in monkey S, the left hemifield was contralesional.

Target-jump trials

These trials were a modified version of the no-jump trials, with FP and T1 at the same locations. The target was displaced (i.e., 'jumped') at the onset of the saccade (defined by the REX online saccade detection algorithm as eye velocity > 100°/s) from its original position (T1) to a new position (T1′) (Fig. 1c, f, h, i). Since we wanted to investigate the neural mechanisms involved in saccadic correction, one goal of the target jumps was to maximize the number of generated CSs. The second purpose of the target jump was to dissociate the PS error and the retinal error signals. Indeed, the displacement of the target introduced a discrepancy between the saccadic error resulting from the PS inaccuracy (the distance of the primary saccade endpoint from T1) and the retinal error (the distance of the primary saccade endpoint from T1′).

Target-jump timing was verified offline using a photocell device placed at the top left corner of the screen, where a light pulse was emitted synchronously with every stimulus transition. T1′ effectively replaced T1 25–45 ms after the onset of the PS, which is essentially due to saccade detector and video hardware response delays. Because this intra-saccadic target jump occurred while the eyes were moving at high velocity, it was probably unnoticed by the monkey due to the 'saccadic suppression' phenomenon preventing

visual feedback from being perceived and influencing the eye trajectory (Bridgeman et al. 1975; Thiele et al. 2002). These trials were randomly interleaved with no-jump trials (final ratio was about 2/3 of trials with target jump). In the single-neuron recording experiment, T1′ could appear at one of two possible locations, in equal proportions: along the PS vector in a forward or backward direction, mimicking target overshoot and undershoot, respectively (see Fig. 1f). The target-jump amplitude represented 25% of the FP–T1 vector in the LIP recording experiment where the final average amplitude of the PSs was 19.6° ± 5°, i.e., equivalent to the PS amplitudes of the no-jump trials (see Table 1). This target jump created an artificial inaccuracy of the PS and ultimately allowed us to "decorrelate" the motor error (difference between the initially programmed PS and the executed PS, programming and execution both based on the initial T1 position before the target jump) and the retinal error (target position visual feedback) after the execution of the PS. In other words, in the case of a trial without target jump (no-jump trials) retinal and motor errors are geometrically equivalent, whereas the intra-saccadic target displacement on the target-jump trials redefines the retinal error, which becomes decoupled from the initial motor error. In the LIP inactivation experiment, the target jump was either backward (centripetal) or forward (centrifugal) relative to the PS direction, and target-jump amplitude was 10% or 20% of the FP to T1 vector, i.e., 1.5° or 3° for 15° saccades and 3° or 6° for 30° saccades. We used different jump directions and amplitudes for two reasons: (1) because monkeys were performing saccades to the same contra- and ipsilesional target positions through the entire duration of the inactivation experiments, varying the target jump served to reduce its predictability and prevent any form of saccadic adaptation. (2) These target-jump values allowed us to cover a range of CS amplitudes, and collect data for CSs falling within the range of the natural corrective saccade amplitude (< 3°) observed in our electrophysiological recording experiment (see below) while keeping a good amount of trials necessitating a large CS (> 3°).

Monkeys executed CSs to compensate for the artificial visual errors created by the target jump. CSs were also observed on no-jump trials, though less frequently. In both the recording and the inactivation experiments, when T1 was displaced, the fixation window shifted instantaneously to match the new T1′ position but its size was unchanged. During recording experiments, the dimension of the eye fixation windows (FP and targets) was a square with side dimensions representing 20% of the vector between FP and T1. In the inactivation experiment, fairly large eye fixation tolerance windows were used, since we could not anticipate the potential effects of muscimol on the accuracy of primary and CSs. Fixation windows were set to ± 40% of the vector between FP and T1 horizontally and ± 20% vertically, centered on T1. Monkeys performed this task at about 80% success rate in both control and inactivation sessions (correct trials/total number of trials including trials where monkeys did not engage the fixation at FP presentation).

Small PS trials

These saccades were used as a control for the direction and amplitude of CS executed in the no-jump and target-jump trials. During recording experiments, visually guided small PSs were made from the central FP to one of four peri-foveal targets. Two targets were positioned at the same retinotopic location as T1′ in the target-jump condition (Fig. 1g for saccade along the axis on the PS), i.e., left or right of the FP. Two other targets were positioned above and below the FP at the same retinal eccentricity as the horizontal targets. This allowed us to fully map the RF of LIP neurons and check for the presence of peri-foveal responses. During inactivation experiments, the FP was placed at ± 22.5° of eccentricity along the horizontal meridian, i.e., halfway between the two different T1 positions in the contra or ipsilesional field. T1 position was set at 2.2° and 4.5° from FP, an eccentricity in the range of the T1′ positions, to match, as closely as possible, the conditions in which CS were made during these experiments. The timing of FP and saccade targets was similar to that used in the no-jump trials.

Statistical analysis

Data analysis was conducted using Matlab (Mathworks Inc., Natick, MA) scripts and Statistica (TIBCO Sofware Inc., Palo Alto, CA). Eye movement data was processed offline to identify saccades by converting horizontal and vertical

Table 1 Mean and standard deviation of latency, duration and amplitude for the primary and corrective saccades of the four types of trials in the single-neuron recording experiments

	Primary saccade			Corrective saccade		
	Latency	Duration	Amplitude	Latency	Duration	Amplitude
No-jump trials without CS	208 ± 33	65 ± 15	19.6 ± 5			
No-jump trials with CS	216 ± 34	66 ± 16	19.9 ± 5	197 ± 92	30 ± 7	2.6 ± 1.7
Target-jump trials	212 ± 31	64 ± 15	19.6 ± 5	174 ± 63	37 ± 6	4.9 ± 1.9
Small PS trials	207 ± 47	36 ± 06	4.6 ± 1.7			

Data are expressed in milliseconds for latency and duration, in degrees of visual angle for amplitude

position traces into velocity traces using five-point differentiation and applying velocity threshold of 30°/s to mark the beginning and end of saccades. Saccade direction and amplitude were defined as the vector difference between eye position at saccade end and start marks. In general, the maximal neural response fields of the recorded neurons were located between 15° and 30° of eccentricity, thus determining the range of PS amplitudes. To analyze post-saccadic activity in relation to motor performance across different trial types (target-jump trials, no-jump trials with and without CSs) and neurons, we quantified saccade accuracy using a normalized accuracy ratio. Though we calibrated the eye position system before each session, constant small offset between the fixated target and the recorded eye position could remain. To avoid any misestimation of actual eye position linked to this potential offset, we used as a reference for the "ideal" saccade, the mean endpoint of PSs on no-jump trials not followed by a CS in each session. We then computed the deviation along the vector of each saccade with respect to this mean endpoint and normalized it to the amplitude of the ideal saccade:

$$\text{Accuracy ratio} = \frac{T - \text{mean (NJT)}}{\text{mean (NJT)}}$$

where T represents single trial (either target-jump, no-jump trials with or without CS) and NJT represents no-jump trials without CS. Note that for target-jump trials, the accuracy ratio refers to the deviation with respect to the original target position (T1), not the displaced one (T1′). This accuracy ratio allowed us to compute the relative motor error of the PSs and thus to consider and compare neurons having different response fields. This is important since a 3° PS inaccuracy would represent an error of 15% for saccade into the center of a response field located at 20° of eccentricity, but an error of 30% for a saccade into the center of a response field located at 10° of eccentricity.

For the single-neuron recording experiment, we computed population-averaged peristimulus and event time histograms (PSTHs) by first obtaining PSTHs (window: 50 ms Gaussian kernel) from each neuron and then computing the mean of these PSTHs. To establish whether cells had visual responses, we compared activity in two 150 ms epochs, before and after T1 onset, in the overlap condition, using a Wilcoxon paired signed-rank test (two-tailed). To establish whether neurons had eye movement-related activity, we compared the mean baseline activity (epoch: − 150 to 0 ms before T1 onset) to the activity following saccade onset (epoch: 50–200 ms) in the overlap task, using Wilcoxon paired signed-rank test (two-tailed). To characterize the spatial tuning of the post-saccadic activity, we computed, for each neuron, a simple spatial selectivity index for the large PSs (Fig. 1d) based on post-saccadic activity (50–200 ms after saccade onset) for saccades in the preferred (always contralateral to the recording site) and anti-preferred direction:

$$\text{Spatial selective index} = \frac{(\text{contralateral FR} - \text{ipsilateral FR})}{(\text{contralateral FR} + \text{ipsilateral FR})}$$

where FR represents the mean firing rate measured after a saccade performed in contralateral or ipsilateral field. The same method was used to characterize the spatial tuning of the post-saccadic neurons following a small PS (Fig. 1g) where we computed the spatial selectivity index by comparing the activity for the small PSs for the same two directions as for the large PSs.

Coefficients of correlation were evaluated using Pearson's linear correlation tests and the difference in proportion of trials using a Chi-squared test. Differences between conditions were assessed by comparing the mean firing rates using Wilcoxon paired signed-rank test (two-tailed). For population analyses, we only included cells in a given comparison when more than five trials were collected in any given condition. Since there were no substantial differences between the patterns of post-saccadic activity and the oculomotor behavior between the two monkeys, we conducted the electrophysiological analyses on data pooled from all recording sessions in the two animals. In view of the number of inactivation sessions ($n = 4$ per monkey), we opted to analyze and present these data separately for the two monkeys. When a trial contained more than one CS, it was not included in the CS analyses. Outlier saccades exceeding three times the standard deviation of the mean saccade latency or diverging by more than 60° of the fixation point–T1 vector were removed from the analyses. Single-neuron recordings and inactivation analyses were carried out using Spearman correlation coefficient, Wilcoxon signed-rank tests (one or two-tailed), Kruskal–Wallis tests (two-tailed), sample paired and unpaired t tests (two-tailed) and ANOVAs for main and interaction effects and pairwise post hoc comparisons (LSD Fisher test), where appropriate (see "Results" section).

Time windows for single-neuron and population data analysis

The selection of spike counting windows for statistical analysis of post-saccadic responses was based on the following rationale. We aligned the neuronal activity on CS onset whenever possible to focus our analyses on the post-PS to pre-CS interval during which no eye movement occurs to rule out any alternative explanation linking observed effects to saccade execution. Because the average latency between the end of the PS and the beginning of the CS was about 174 ms (Table 1 of our manuscript), using a window of 150 ms starting 150 ms before CS onset was the best way to compare the neural activity during trials with different PS

accuracies while making sure that none of the differences observed can be linked to a motor execution of the PS or the CS.

When aligning on PS onset, we also used a 150 ms window from 50 to 200 ms after PS onset. This allows us to keep the same window length than the analyses with CS alignment (i.e., 150 ms) while (a) rejecting most of the epoch of the PS execution (average duration 64 ms, see Table 1) and (b) keeping most of the relevant post-saccadic activity before the execution of the CS. To evaluate the effects of PS accuracy on trials with no intra-saccadic trial jump (no-jump trials), we had to align activity on PS onset because these analyses included a substantial number of trials without a CS. To be consistent in the other analyses, we kept window lengths of 150 ms, using early (0–150 ms) and late (150–300 ms) PS onset-aligned windows to show that differences between different trial types are found later, in keeping with the longer latency of CS decisions on no-jump trials.

Results

We first present the results from the single-neuron recording experiment followed by those of the reversible inactivation experiment.

Saccadic behavior

To analyze and meaningfully interpret post-saccadic neuronal responses, we first characterized the saccadic behavior in four trial types (Table 1). PS amplitudes in our data range from 15° to 30° with an average around 20°. Consistent with previous findings in humans (Becker 1972, 1991), PS latencies were longer than those of CSs. For example, when matching the saccadic amplitude by comparing PSs to peri-foveal targets with CSs, CS latencies were significantly shorter (207 ms vs. 174 ms for small PS condition and CS of target-jump trials, respectively, $t(4638) = 20.2274$; $p < 1 \times 10^{-3}$; unpaired t test). This was true despite PS to peri-foveal targets being, on average, slightly smaller than CS (4.6° vs. 4.9° for small PS condition and CS of target-jump trials, respectively, $t(4638) = 6.0239$; $p < 1 \times 10^{-3}$).

We used an accuracy ratio (see "Methods") to represent the primary saccade endpoint error normalized by its amplitude (i.e., a proportional error: Fig. 2a). We defined as 'most accurate trials', trials with PS falling within the ±0.02 accuracy ratio range. Note that these saccades could also be defined as having a gain superior to 0.98, since the gain is traditionally defined as the ratio of the actual saccade amplitude divided by the desired saccade amplitude (1–0.02 = 0.98 where 1 represents the PSs foveating optimally T1 in our accuracy ratio, i.e., the desired saccade, and 0.02 the actual accuracy ratio cutoff related to the deviation from these desired saccades). We further defined groups of saccades based on non-overlapping accuracy threshold ranges to increase statistical power and maximize accuracy ratio differences between the different groups (e.g., high- vs. low-accuracy trials): low-accuracy hypometric (35.5% in no-jump condition) and hypermetric (35.5%) trials with accuracy ratio inferior to −0.02 and superior to 0.02, respectively, and high-accuracy trials (29%). As expected, for the no-jump condition the proportion of trials on which a CS occurred increased as a function of the unsigned accuracy ratio of the PS (Fig. 2b; $r = 0.899$, $p < 1 \times 10^{-4}$, $n = 12$, Pearson's correlation test). The amplitudes of the CSs on no-jump trials also increased with PS inaccuracy, i.e., with the size of the unsigned accuracy ratio (Fig. 2c; $r = 0.67$, $p < 1 \times 10^{-49}$, $n = 379$, Pearson's correlation test). Note that CSs were generated also on most accurate trials (i.e., ±0.02 range) in the no-jump trials. These CSs had the smallest amplitudes (about 2° on average, Fig. 2c) but also the longest CS latencies (e.g., ~230 ms vs. ~155 ms for most accurate and inaccurate trials, respectively, $t(71) = 4.1248$, $p < 1 \times 10^{-4}$, $n = 73$, unpaired t test (two-tailed); all trials, $r = -0.22$, $p < 1 \times 10^{-4}$, $n = 379$, Pearson's correlation test, Fig. 2d). These observations match previous results (Becker 1972, 1976; Deubel et al. 1982) showing that the CS latency decreases and the probability of performing a CS increases with the amplitude of the saccadic error. On target-jump trials, the accuracy ratio refers to the error of the PS relative to the pre-jump target position (T1), whereas the CSs are directed towards the new target position (T1′), thus precluding conducting similar analyses.

Single-neuron recordings from LIP

Response characteristics of post-saccadic neurons

Out of a total of 90 neurons ($n = 49$ and $n = 41$ for monkeys N and S) that responded during the visual, delay or saccadic phase of the overlap saccade task, one-third ($n = 30$) showed the classical LIP pattern of visuo-saccadic activity (Fig. 3a), responding both to the target onset and around saccade execution. We also recorded neurons with visual selectivity for the target or fixation point as well as neurons without clear modulation in any of the experimental tasks ($n = 26$). Since we were interested in LIP neural correlates of an error signal after the PS, our analyses focused on the remaining subset of 34 post-saccadic neurons (21 in monkey N and 13 in monkey S). Importantly, the responses of these neurons were only post-saccadic and were not visually modulated by the target onset in their RF (Fig. 3b). These post-saccadic neurons were anatomically intermingled with the other LIP recorded neurons (see Fig. 1a) and no specific pattern of distribution was observed over the recording area. The presence of post-saccadic neurons in the vicinity of visual and

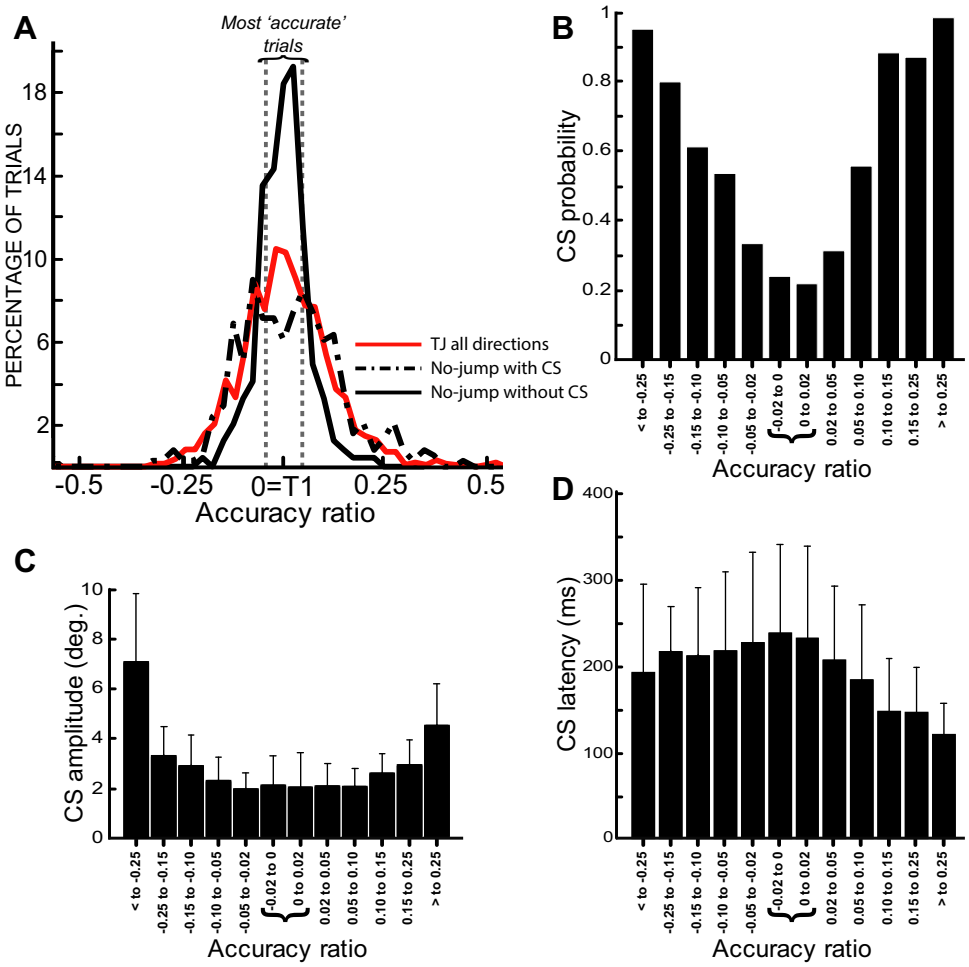

Fig. 2 Saccadic behavior. **a** Distribution of primary saccade accuracy ratios for no-jump trials with and without CS and for target-jump trials. Note that the 'Most accurate trials' range (accuracy ratio between −0.02 and 0.02) refers to the accuracy of the PS relative to T1, not T1′, for all trial types. **b**–**d** represent, respectively, the probability of occurrence, amplitude and latency of CS as a function of PS accuracy, for no-jump trials. Columns and error bars represent mean and standard deviation

pre-saccadic cells in LIP is consistent with previous work (Zhou et al. 2016). However, the relatively high proportion of such cells in our data set (38%) should not be considered as an unbiased estimate of their actual prevalence in LIP as our sampling of LIP cells was deliberately guided by an a priori interest in post-saccadic activity. Thus neurons with post-saccadic activity were specifically searched.

Post-saccadic neurons responded after both small and large PSs in their preferred direction. As expected, the neural modulation was stronger after the large saccades made into the response fields of the neurons (Fig. 3c, red and blue curves for neural responses of large and small PS conditions, respectively; Fig. 3d; $z=4.0262$, $p<1\times10^{-4}$; $n=34$, signed-rank test). On target-jump trials, the large PS was followed by a CS with end points similar to those of the small PS. However, the neural responses to the CSs were weaker than the responses of the equivalent-size small PSs (Fig. 3e, red curve for target-jump trials aligned on corrective saccade onset vs. blue curve for small PSs aligned to PS onset; Fig. 3f, $z=3.1885$, $p=0.0014$, $n=34$, signed-rank test). The activity relative to CS execution in target-jump conditions remained significantly larger than baseline activity ($z=3.6004$, $p<1\times10^{-3}$, $n=34$, signed-rank test). Because these saccades were performed at similar location on the screen, the difference found in post-saccadic response for CSs and small PSs indicates that the response is not merely related to the saccade metrics or to an orbital eye position signal, both of which remained constant between the two conditions. Since the amplitudes of the small PSs and CSs are equivalent (Table 1), the higher activity following the small PSs (but much smaller than the activity related to large PSs, Fig. 3) suggests that LIP post-saccadic neurons are primarily involved after the execution of the first saccade of a saccadic sequence. However, the post-saccadic activity after the completion of the CSs (following a large PS) being higher than the baseline level suggests that the LIP post-saccadic neurons remain involved for the entire saccadic sequences until completion of the saccadic goal, i.e., the foveation of the target.

Also the spatial selectivity index clearly showed that post-saccadic activity for large contraversive saccades was higher than that for large ipsiversive saccades (Fig. 3h, mean index $=0.346$, $z=3.0005$, $p=0.0027$, $n=34$, signed-rank test). Therefore, the preferred direction of the saccades is

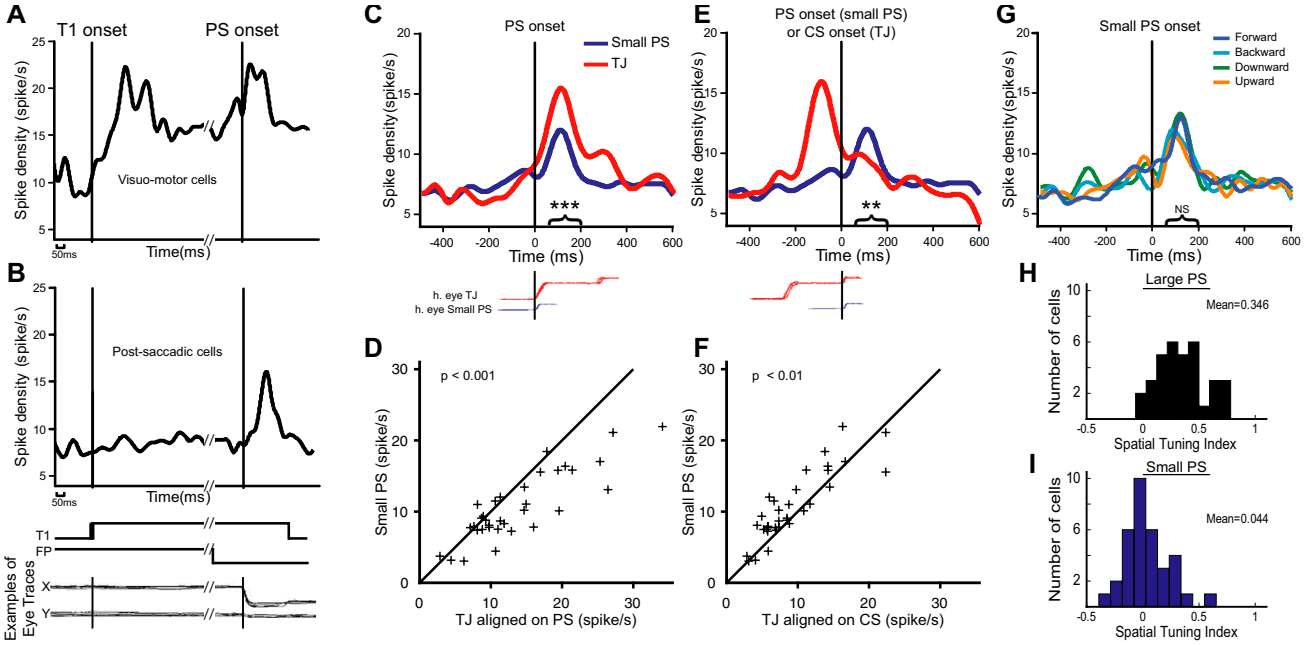

Fig. 3 Neural activity in LIP after visual stimulation and saccadic eye movement. **a** In the overlap control task, a first population of visuo-motor neurons ($n=30$) showed an increase of activity for T1 onset and PS execution. **b** The post-saccadic neurons ($n=34$) showed an increase of activity only after the saccade onset. Calibration bars on the *x*-axis represent 50 ms. **c–f** Neural responses related to saccadic execution as a function of saccadic amplitude. **c** Population response curve of post-saccadic neurons in target-jump (red curve) and small PS (blue curve) conditions aligned on PS onset. The amplitudes and directions of PS in small PS condition are equivalent to those of the CS in target-jump condition. Asterisks indicate significance between the two conditions in the epoch indicated by the brackets ($^{**}p<0.01$). D shows the distribution of mean response of each neuron and signed-rank statistical results over the post-saccadic population for Fig. 2c (epoch 50–200 ms) for target-jump vs. small PS conditions. **e** Same activity than **c** but aligned on PS for small PS condition and on CS for target-jump condition ($^{***}p<0.001$). **f** The distribution of mean response of each neuron and signed-rank statistical results over the post-saccadic population for **e** (epoch 50–200 ms) for target-jump vs. small PS conditions (here the activity for target-jump trials corresponds to the time of the CS). **g** Post-saccadic population response curve for to the four small PS conditions. Activity is not significantly between the four directions ('NS' for non-significant signed-rank test, $p>0.05$). **h** Spatial tuning of post-saccadic neuron for large PS in contralateral (preferred) vs. ipsilateral (anti-preferred) directions. Here, neurons respond more strongly for contraversive than ipsiversive saccades (mean = 0.346). **i** Spatial tuning for small amplitude PS in preferred vs. anti-preferred direction. Most cells show little or no directional preference for small contraversive and ipsiversive saccades (mean = 0.044)

towards the contralateral field. In contrast, post-saccadic activity for small PSs did not depend strongly on the saccade direction (Fig. 3g, $X^2(3,132)=2.29$, $p=0.5144$, $n=34\times4$, Kruskal–Wallis test). On average, the neural response for small saccades in the same direction as the neuron's response field was equivalent to the neural response for small saccades in the opposite direction (Fig. 3i, mean index = 0.044, $z=1.2329$, $p=0.2176$, $n=34$, signed-rank test). These data show that this post-saccadic population is spatially best characterized by a large contralateral response field (mean index of 0.346 for large PS vs. mean index of 0.044 for small PS, $z=4.1801$, $p<1\times10^{-4}$, $n=34$, signed-rank test), which also includes the ipsilateral peri-foveal region. Despite the fact that the neurons' response field was only partially mapped, these results suggest that the post-saccadic response fields may include the peri-foveal region but are mainly centered on large eccentricities since their preferential direction is clearly towards peripheral targets contraversive to the recorded hemisphere.

Post-saccadic activity is higher after low-accuracy primary saccades

The purpose of a CS is to fine-tune foveation of the target. Under natural conditions (i.e., without intra-saccadic target jumps), the amplitude of the CS is correlated with PS accuracy since the magnitude of the PS motor error determines the retinal error that the CS will aim to reduce. As a result, on no-jump trials, the inaccuracy of the PS could be detected by the oculomotor system through any of three possible mechanisms: a re-afferent retinal signal indicating the retinal location of the target after the saccade, a motor error signal computed from the efference copy of the motor command (Sommer and Wurtz 2008) or a proprioceptive eye position signal which could be conveyed via the eye representation in primary somatosensory cortex (Wang et al. 2007). In contrast, in the target-jump condition, the displacement of the target during the execution of the PS dissociates retinal feedback from the other two sources, since the former

provides information about the post-displacement target position while the latter would indicate the error relative to the original target position (i.e., the "desired" endpoint of the PS).

We initially classified individual target-jump trials according to PS accuracy: trials in which the PS had an accuracy index between − 0.02 and 0.02 were classified as high-accuracy PSs (equivalent to an average absolute error below 0.4°; mean accuracy ratio = 0.01 for these trials which is equivalent to 0.2°), and the trials with unsigned accuracy ratio greater than 0.02 as low-accuracy PSs (mean accuracy ratio = 0.1, i.e., equivalent to an average absolute error of 2°, see Fig. 2a and Table 1). Because CSs were heavily represented in the target-jump condition (> 80% of trials across all session) we could align the response of post-saccadic neurons to the onset of the CS, thereby enabling us to establish whether post-PS activity occurred primarily before, in conjunction with or after CS execution. The results show that inaccuracy of the PS is signaled in LIP by enhanced activity of post-saccadic neurons. As shown in a single-neuron example presented in Fig. 4a, activity was significantly higher for low-accuracy PSs compared to high-accuracy PS. At the population level, this effect was observed in the interval between the end of the PS and the onset of the CS (Fig. 4b, window was set from − 150 to 0 ms before CS onset, $z = -2.1715$, $p = 0.0299$, $n = 26$, signed-rank test, note that average inter-saccadic latency between PS and CS was 174 ms in target-jump condition, see

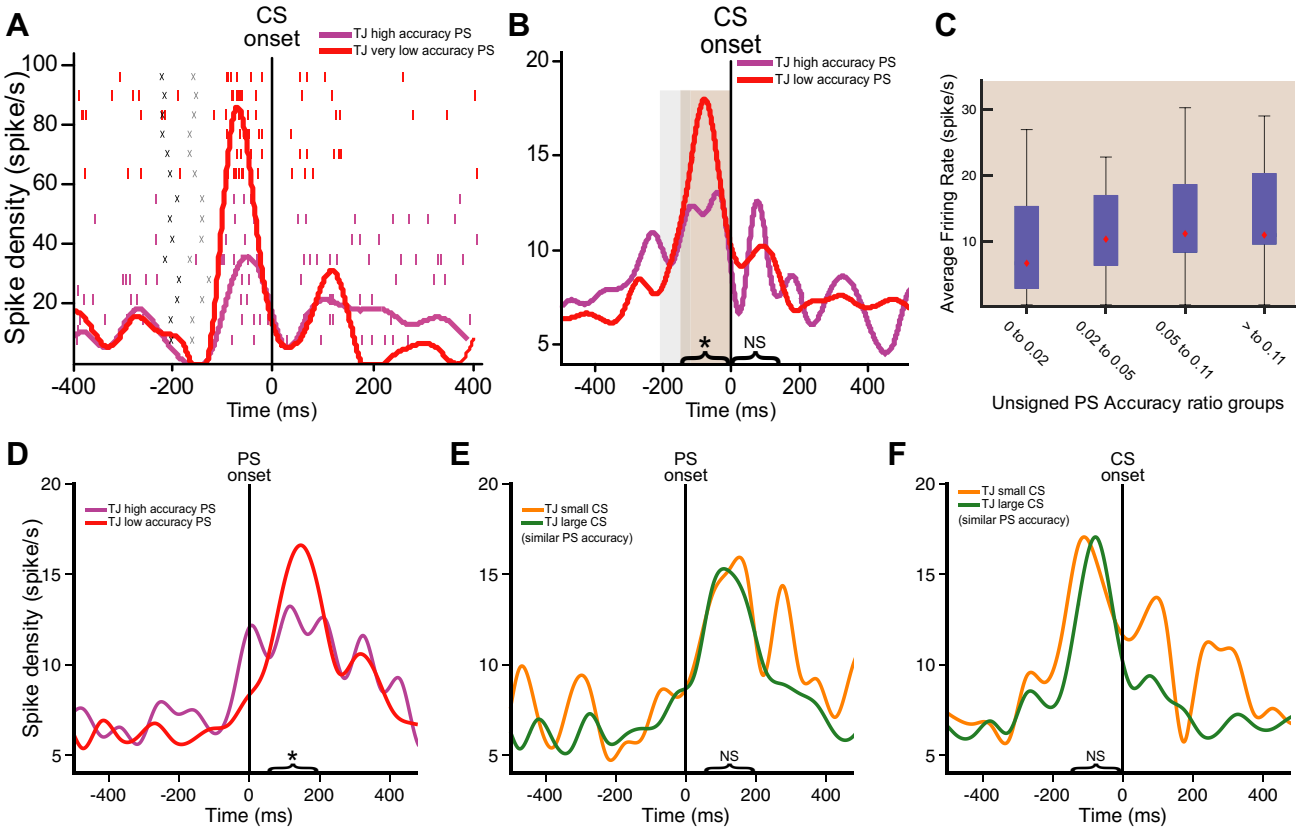

Fig. 4 Post-saccadic activity as a function of primary saccade accuracy. **a** PSTH and raster plot of a typical neuron aligned on CS onset during target-jump trials with very low and high PS accuracy ratio. Red for lowest PS accuracy trials (accuracy ratio > 0.1) and purple for highest PS accuracy trials (< 0.02). Each raster line represents a trial. Black and gray crosses represent, respectively, the beginning and end of PSs (amplitude: 14.6° ± 0.17 and 14.4° ± 1.14 for PSs with low- and high-accuracy ratio, respectively). **b** Average neural response for low (mean = 0.1 ± 0.05) vs. high (mean = 0.01 ± 0.004) PS accuracy ratio. Epoch preceding CS execution (window: − 150 to 0 ms before CS onset, brown-shaded area) shows a stronger neural response for low than for high accuracy. Time range of PS ending is indicated by the gray shaded area. **c** Average neural activity as a function of PS accuracy before CS onset (− 150 to 0 ms). Each bar represents about 20–30% of the trials (high, medium, poor, very poor accuracy from left to right). Red diamonds represent median, blue bars and whiskers represent 75th and 99th percentiles, respectively. **d** Same average neural response as in **b** but aligned on PS onset (analysis window: 50–200 ms after PS onset). **e**, **f** Post-saccadic activity aligned on the onset of the PSs (**e**) or of the CSs (**f**) as a function of primary saccade accuracy. Average neural response for large (mean = 5.6°) vs. small (mean = 2°) CS trials after the execution of the PS are similar when the PS accuracy ratio (means: 0.09 for large CS trials, 0.11 for small CS trials) is equivalent (analysis windows: 50–200 ms after PS onset, **e**; − 150 to 0 ms before CS onset, **f**). Note that for each panel, neurons included in each analysis contained more than five trials. Asterisks indicate significance between condition (*$p < 0.05$), 'NS' for non-significant signed-rank tests

Table 1). No difference was found after CS onset (0–150 ms after CS onset, $z = -0.9552$, $p = 0.3395$, $n = 26$, signed-rank test). Aligning the neural activity at the onset of the PSs yields essentially the same result with a neural activity significantly lower for the highly accurate trials 50 ms after the onset on the saccade (i.e., around the end of the PS; Fig. 4d, analysis window: 50–200 ms after PS onset, $z = -2.0192$, $p = 0.0435$, $n = 26$, signed-rank test). In the light of this result, we next asked whether this effect of saccade accuracy on neuronal activity is proportional to the size of the saccadic errors. We subdivided the trials into four blocks according to their accuracy ratio (i.e., ≈20–30% of trials per group, see Fig. 4c) and found that post-saccadic neural activity difference tends to increase with the inaccuracy of the PS (Fig. 4c, three-step difference of accuracy ratio: high vs. very poor accuracy, $z = -2.3517$, $p = 0.0093$; two-step difference: high vs. poor, $z = -1.9908$, $p = 0.0233$; medium vs. very poor, $z = -0.8276$, $p = 0.2040$; one-step difference: high vs. medium, $z = -1.3705$, $p = 0.0853$; medium vs. poor, $z = -1.0889$, $p = 0.1381$; poor vs. very poor, $z = -0.3485$, $p = 0.3637$; $n = 18$, one-tailed signed-rank test. With the application of a very stringent (in the context of a priori comparisons) Bonferroni correction of the alpha level ($0.05/6 = 0.0083$), none of these pairwise comparisons remained significant. However, the Spearman correlation computed on the same data was significant ($r = 0.2143$, $p = 0.0353$, $n = 18$ neurons × 4 accuracy groups), thus revealing the existence of a trend for the post-saccadic response to augment in conjunction with the motor error size. Critically, in the presence of an intra-saccadic target jump, the amplitude of the retinal error and the subsequent CS are no longer linked to PS accuracy, since the CS is directed towards the displaced target. Thus, this effect of PS accuracy was not due to the re-afferent retinal signal, because the retinal error (distance from the PS endpoint to the location of the displaced target) was in fact on average similar for both high- and low-accuracy PSs (4.8° ± 1.5 and 5.1° ± 2.3, respectively) as were the CS latencies (164 ms ± 59 and 171 ms ± 68, respectively). This is possible because, on one hand, a hypometric PS with an intra-saccadic backward or forward target jump induced, respectively, a small or large retinal error before the CS (and inversely for a hypermetric PS). On the other hand, an accurate PS with the same backward and forward target-jumps results in a medium retinal error.

Finally, additional analyses show that the post-saccadic activity after the PS execution is not modulated as a function of the absolute retinal errors (< to 3° or > to 3°, Fig. 4e, f) when the PS motor error (accuracy ratio) is similar. Indeed, we found no statistical difference between the trials with large (5.6° ± 1.04) or small (2° ± 0.48) CSs despite there being a similar PS accuracy ratio (0.09 ± 0.06 for large CS trials, 0.11 ± 0.06 for small CS trials) (analysis windows: 50–200 ms after PS onset—Fig. 4e, $z = -0.0601$, $p = 0.9521$; −150 to 0 ms before CS onset—Fig. 4f; $z = -0.7239$, $p = 0.4691$; $n = 27$, signed-rank test). Note that the difference after the CS onset in Fig. 4f can be attributed to the large CSs performed in the anti-preferred direction of the neurons which lower the response after the CS execution for the large CS trials. Therefore, these results reinforce the conclusion that the post-saccadic neurons are modulated by the amplitude of the PS motor error.

Post-saccadic modulation after primary saccades can probably not be attributed to other factors than primary saccade motor error

To further confirm the dependence of post-saccadic activity on PS accuracy, we first compared the activity of no-jump trials with or without CS as a function of the PS accuracy ratio. Here, we opted to align neuronal activity on PS onset because on such trials CS are much less frequent than on target-jump trials (≈1/3 of no-jump trials across all sessions) and we wished to compare neuronal activity on trials associated with PS errors of the same size that are followed or not by a CS. Immediately after the onset of the PS, post-saccadic neural activity was not significantly different between low- and high-accuracy trials (Fig. 5a, early epoch: 0–150 ms, $z = 0.5433$, $p = 0.5869$, $n = 21$, signed-rank test). However, 150–300 ms after PS onset, the neural response for these trials was significantly modulated by the accuracy of the PS since the neural activity in no-jump trials returned to baseline earlier on high-accuracy trials compared to low-accuracy trials (Fig. 5a, late epoch: 150–300 ms, $z = -2.0336$, $p = 0.0420$, $n = 21$, signed-rank test. Note that the average CS latency is longer for the no-jump trials than for the target-jump trials, see Table 1, and note also that an inaccurate PS may not be followed by a CS probably because the large tolerance window allows monkeys to be rewarded without hyper-precise foveation of the target. It is thus possible that the late enhanced activity on these no-jump trials reflects the 'uncertainty' of the oculomotor system as to the necessity of correcting for an inaccurate PS. These results confirm that the inaccuracy of the PS is also signaled under natural conditions (i.e., during no-jump trials with or without CS) by an enhanced activity in post-saccadic LIP neurons. Importantly, the difference between accurate and inaccurate saccades was not associated with the preparation of a CS after an inaccurate PS. Indeed, there was no significant difference between the activity on low-accuracy trials with and without a CS (Fig. 5b, activity tested from 0 to 150 ms after PS onset, $z = 1.1314$, $p = 0.2579$; 150–300 ms after PS onset, $z = 0.6275$, $p = 0.5304$; $n = 31$, signed-rank test). Moreover, there was still a difference, although marginal probably due to the lack of statistical power in this very restrictive analysis, between the activity of high-accuracy trials without CS (we removed the few trials with a CS in this trial

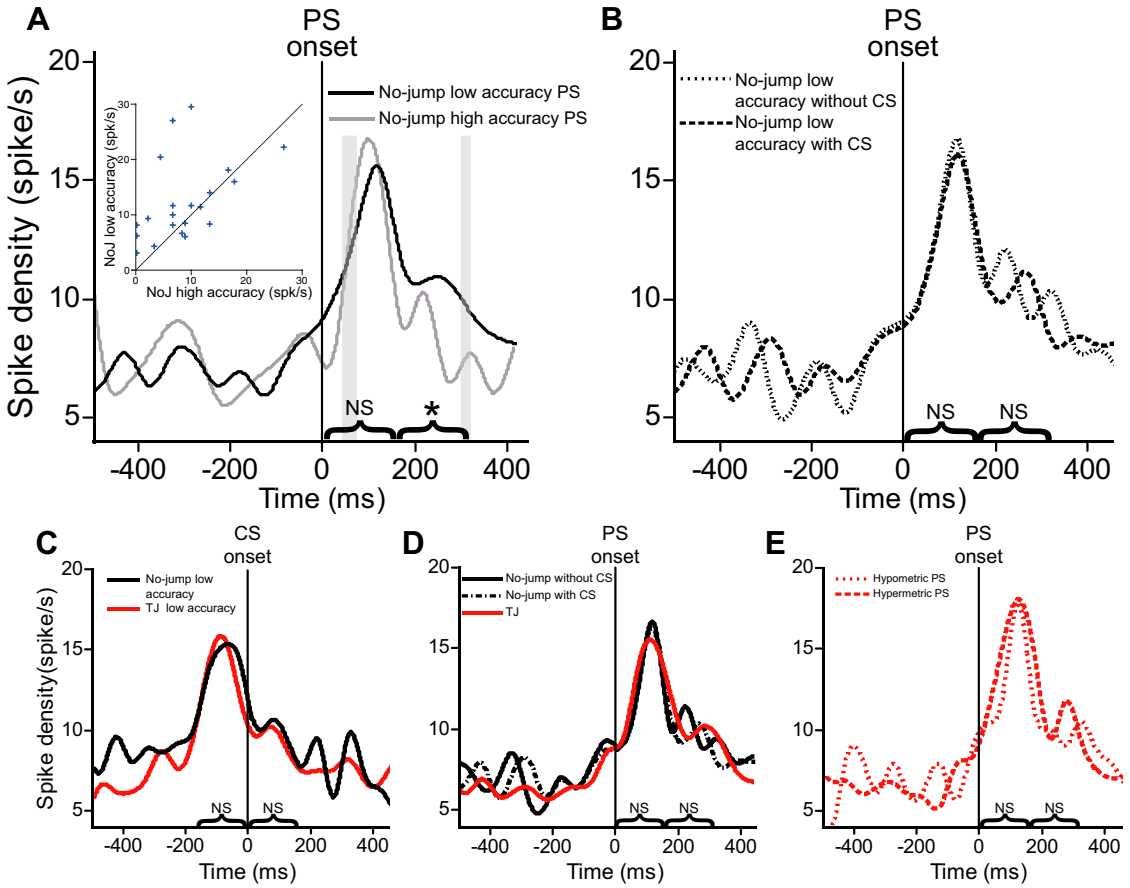

Fig. 5 Post-saccadic modulation is best explained by the primary saccade's accuracy. **a** Post-saccadic average neural response aligned on PS onset for low- vs. high-accuracy ratio on no-jump trials (with and without CS). The neural response of low-accuracy trials is higher in the late epoch (150–300 ms after PS onset) compared to high-accuracy trials. The two shaded areas indicate the time range of PS (left) and CS (right) ending. Small scatter plot inset represents mean firing rate of individual neurons for no-jump trials with high vs. low PS accuracy in the statistically significant window. **b** Average neural responses for no-jump trials with low accuracy as a function of CS occurrences. Data are aligned on PS onset. **c** Average neural responses of low PS accuracy trials for No-jump with CS and target-jump trials (accuracy ratio between >0.02 and <0.1). Data are aligned on CS onset. **d** Average neural response for no-jump trials with and without CS and for target-jump trials. Data are aligned on PS onset. **e** Average neural responses for trials in target-jump condition as a function of the direction of PS error. Data are aligned on PS onset. Dashed and dotted curves represent, respectively, largely hypermetric (i.e., accuracy ratio >0.05) and hypometric (i.e., accuracy ratio <-0.05) trials. For all these analyses, no difference was found for any of the epochs proceeding or following CS or PS. Note that for each panel, neurons included in each analysis contained more than five trials. Asterisks indicate significance between condition ($*p<0.05$) for signed-rank test, 'NS' for non-significant tests

type) and low-accuracy trials without CS (activity tested from 0–150 ms after PS onset, approximate $z=-0.4707$, $p=0.6379$; 150–300 ms after PS onset, approximate $z=-1.6499$, $p=0.099$; $n=13$, signed-rank test).

We next compared the activity aligned to the CS onset for no-jump and target-jump trials with low-accuracy ratio [i.e., ratios between 0.02 and 0.1; mean = 0.057 (± 0.2) and 0.056 (± 0.2) for the no-jump and target-jump conditions, respectively]. Neural responses in these two types of trials were enhanced prior to CS onset and did not differ statistically (Fig. 5c, −150 ms to CS onset, $z=-1.3477$, $p=0.1778$; 0–150 ms after CS onset, $z=-1.3323$, $p=0.1828$; $n=32$, signed-ranked test), further confirming that this neural modulation is dependent on the execution and metrics of the PS, and not to the re-afferent retinal feedback, which differs between the two task conditions (note that using very poor accuracy PS instead of low accuracy yield similar results, although fewer neurons can be used for this analysis). In fact, the activity of these neurons appears insensitive to the intra-saccadic target manipulation since the average activity of the population does not differ between no-jump trials (with or without a CS) and target-jump trials (Fig. 5d, 0–150 ms after PS onset, $X^2(2, 93)=0.4502$, $p=0.7984$; 150–300 ms after PS onset, $X^2(2, 93)=0.4381$, $p=0.8033$; $n=32\times3$, Kruskal–Wallis test). Finally, there was no significant difference in activity depending on whether the saccadic error was due to large undershooting or overshooting of the target position (Fig. 5e, 0–150 ms after PS onset: $z=-1.2140$,

$p = 0.2247$; 150–300 ms after PS onset: $z = -1.0783$, $p = 0.2809$; $n = 31$, signed-rank exact). Hence, the modulation observed was associated to the size but not to the direction of the error. The modulation was also not associated to saccade statistics like the amplitude or the duration of the PS, since overshooting (hypermetric) PSs are by definition larger and longer compared to the undershooting (hypometric) PSs.

Taken together, these neurophysiological results suggest that post-saccadic LIP neurons signal the motor error magnitude relative to the execution of the PS but neither the size of the retinal post-saccadic error, nor the preparation of a CS to compensate this error.

Causal relation between LIP neural activity and saccadic performance: effects of LIP inactivation

We next tested the hypothesis that LIP plays a functional role in saccadic error processing by unilaterally inactivating this area using muscimol, a GABA agonist. We predicted that, despite our finding that the activity of LIP post-saccadic neurons does not predict CS initiation, the error signals carried by these cells contribute to the execution of corrective mechanisms. Furthermore, another class of cells described by Zhou et al (2016) does show later activity that is modulated according to CS probability, further suggesting that LIP inactivation might impair CS generation. As pointed out in the Introduction, small (< 3°) and large (> 3°) saccadic corrections may compensate errors that have different origins and are generated via different mechanisms (Becker 1991). Small CSs, which represent the majority of the CSs in the recording experiment (see Fig. 2a, c), result from an error of execution (instead of planning error) and cannot therefore be predicted before the end of the PSs. We therefore used the target-jump paradigm, which allows to induce many CSs within a broad amplitude range, to analyze the effects of inactivation on small vs. large CSs. We predicted that inactivation effects would be most prominent for small than large CSs, since the former are most likely to engage a process of whether the residual retinal error of the target can be tolerated or not by the visual system.

Small increase in primary saccade latency to contralesional targets

Muscimol inactivation increased the latency of the PS to contralesional targets for both monkeys (Table 2A). In monkey N, the effect was very small but significant (+5 ms at 15° and +8 ms at 30°; unpaired t test (two-tailed): for 15° T1, $t(338) = -2.002$, $p = 0.0461$; for 30° T1, $t(255) = -2.555$, $p = 0.0112$). The impairment was more substantial in monkey S (+26 ms at 15° and +28 ms at 30°; unpaired t test (two-tailed): for 15° T1, $t(260) = -5.9886$, $p < 1 \times 10^{-6}$; for 30° T1, $t(246) = -5.2692$, $p = p < 1 \times 10^{-6}$). In contrast, inactivation had no significant effect on PS accuracy to contralesional targets, with the single exception of a 0.36° difference for 15° T1 saccades in monkey S [unpaired t test (two-tailed); monkey N, for 15° T1, $t(338) = 0.9227$, $p = 0.3568$; for 30° T1, $t(255) = 0.4219$, $p = 0.6734$; monkey

Table 2 Results for primary saccades on target-jump trials to contralesional (A) and ipsilesional (B) targets in control vs. inactivation sessions

A. PS to contralesional targets

	T1 ECCENTRICITY - CONTRALESIONAL								
	15°				30°				
	CONTROL		INACTIVATION		CONTROL		INACTIVATION		
Latency	238 ±21	*	243 ±24		214 ±29	*	222 ±23		Monkey N
Accuracy	4.31 ±2.38		4.57 ±2.8		5.18 ±2.29		5.31 ±2.53		
Latency	211 ±37	***	237 ±33		230 ±38	***	258 ±44		Monkey S
Accuracy	1.76 ±1.12	**	1.40 ±1.13		2.56 ±1.75		2.53 ±1.83		

B. PS to ipsilesional targets

	T1 ECCENTRICITY - IPSILESIONAL			
	15°		30°	
	CONTROL	INACTIVATION	CONTROL	INACTIVATION
Latency	175 ±20	177 ±22	2.54 ±0.7	269 ±42	Monkey N
Accuracy	2.47 ±0.72	2.38 ±0.74	4.41 ±1.5	4.57 ±1.51	
Latency	251 ±57	254 ±57	224 ±38	224 ±50	Monkey S
Accuracy	2.56 ±0.69	2.54 ±0.7	4.56 ±1.51	4.61 ±1.5	

Latencies are in milliseconds, accuracy (residual error) in degrees. Font types indicate significant differences for unpaired t test (* for $p < 0.05$, ** for $p < 0.01$, *** for $p < 0.001$; ± for standard deviation)

S, for 15° T1, $t(260) = -2.6134$, $p = 0.0095$; for 30° T1, $t(246) = -0.1185$, $p = 0.9058$; Table 2A]. Inactivation had no impact on the performance of PS towards ipsilesional targets [unpaired t test (two-tailed); monkey N, for 15° T1, $t(297) = 0.6657$, $p = 0.5061$ and $t(297) = -1.1495$, $p = 0.2513$ for latency and accuracy, respectively; for 30° T1, $t(227) = 1.1494$, $p = 0.2516$ and $t(227) = 0.8411$, $p = 0.4012$; monkey S, for 15° T1, $t(213) = 0.4320$, $p = 0.6662$ and $t(213) = -0.2478$, $p = 0.8045$; for 30° T1, $t(197) = -0.0036$, $p = 0.9971$ and $t(197) = 0.2474$ $p = 0.8049$; Table 2B].

As described previously, large errors (with magnitude > to 3°) lead almost systematically to the execution of a CS. This is not the case for smaller errors, even though small CSs performed to compensate a PS error below 3° represented 75% of all CSs made on no-jump trials [see Fig. 2b, c and (Becker 1991)]. This indicates that the oculomotor system is finely tuned to respond within this error range since most of the natural motor variability fall under this 3° boundary. It is therefore possible that two distinct corrective mechanisms are used to perform CSs compensating PS error falling, respectively, above and below 3°. We used this cutoff to guide our data analysis. This choice of 3° is also consistent with previous results showing that a PS bringing the target within a 3° radius around the fovea does not automatically generate a CS, because this accuracy is sufficient to allow a correct visual perception (Becker 1991). Therefore, we performed separate statistical analyses on small and large CSs following PSs to contralesional and ipsilesional targets.

No consistent inactivation effect on the probability of executing a corrective saccade or on corrective saccade accuracy.

Overall, LIP inactivation did not change the likelihood of CSs on target-jump trials (Chi-squared test; monkey N: 88% vs. 85% between inactivation and control sessions, respectively, following a contraversive PS, $X^2 = 1.3992$, $p = 0.2369$, $n = 323$ inactivation trials, $n = 369$ control trials; monkey S: 61% vs. 56%, $X^2 = 2.0124$, $p = 0.1560$, $n = 412$, $n = 461$).

However, splitting the CSs by their amplitude shows that the probability of executing a small CS was inconsistent between monkeys since it was unaffected in monkey N (Chi-squared test; 23.5% of trials with small CS during inactivation vs. 22% during control, $X^2 = 0.2446$, $p = 0.6209$, $n = 323$ inactivation trials, $n = 369$ control trials) but increased during inactivation for monkey S (17.5% of trials with small CS during inactivation vs. 10% during control, $X^2 = 11.0711$, $p < 1 \times 10^{-3}$, $n = 412$ inactivation trials, $n = 461$ control trials). The probability of performing a large CS remained unchanged for the two monkeys (monkey N: 64.5% vs. 63%, $X^2 = 0.1727$, $p = 0.6777$, $n = 323$ inactivation trials, $n = 369$ control trials; monkey S: 43% vs. 46%, $X^2 = 0.7918$, $p < 0.3735$, $n = 412$ inactivation trials, $n = 461$ control trials).

Also, LIP inactivation did not lead to a significant change in CS accuracy, since the residual error towards the target remained unchanged [Table 3; ANOVA, Monkey N, for 15° T1: $f(1,336) = 0.6586$, $p = 0.4176$, for 30°

Table 3 Latency and accuracy (residual error) of CS during target-jump trials after contraversive 15° and 30° PS (A) small CS (< 3°) in control vs. inactivation sessions and (B) large CS (> 3°) in control vs. inactivation sessions

A. Small CS

	T1 ECCENTRICITY								
	15°				30°				
	CONTROL		INACTIVATION		CONTROL		INACTIVATION		
Latency	125 ±21	***	143 ±30		154 ±35	**	199 ±58		Monkey N
Accuracy	0.40 ±0.32		0.41 ±0.29		0.66 ±0.56		0.80 ±0.55		
Latency	288 ±58	**	329 ±62		258 ±41	*	322 ±63		Monkey S
Accuracy	0.97 ±0.78		0.88 ±0.9		1.32 ±0.59		1.49 ±0.44		

B. Large CS

	T1 ECCENTRICITY				
	15°		30°		
	CONTROL	INACTIVATION	CONTROL	INACTIVATION	
Latency	110 ±16	111 ±18	139 ±40	148 ±50	Monkey N
Accuracy	0.43 ±0.30	0.38 ±0.27	1.08 ±0.65	1.35 ±0.65	
Latency	289 ±62	286 ±65	270 ±73	276 ±71	Monkey S
Accuracy	1.53 ±0.66	1.49 ±0.88	1.56 ±0.65	1.38 ±0.73	

Left and right panels represent results for monkey N and S, respectively. Latencies are in milliseconds, accuracies in degrees. Interaction effect (inactivation X CS amplitude) was significant for 15° and 30° saccades in both monkeys. Post hoc analyses showed significant effects only for small CS latency (* for $p < 0.05$, ** for $p < 0.01$, *** $p < 0.001$; ± for standard deviation)

T1, $f(1,253) = 0.3776$, $p = 0.5395$; Monkey S, for 15° T1: $f(1,258) = 0.08344$, $p = 0.7729$, for 30° T1, $f(1,244) = 1.9146$, $p = 0.1677$].

Inactivation mainly perturbs small corrective saccade latency following contraversive saccades and had no effect on the corrective saccades performed in the ipsilateral field

In both monkeys, LIP inactivation led to an increase in the latency of small CSs following contraversive PSs (Table 3A). This effect was highly consistent: it was present in both monkeys for both PS amplitudes. In contrast, LIP inactivation did not have any significant effect on large CSs (Table 3B) [ANOVA, Monkey N, for 15° T1: $f(1,336) = 12.234$; $p < 1 \times 10^{-3}$, LSD Fisher post hoc test: small CS (inactivation vs. control), $p < 1 \times 10^{-5}$, large CS, $p = 0.496$; for 30° T1, $f(1,253) = 5.92$, $p = 0.0157$, LSD Fisher: small CS, $p = 0.0011$, large CS, $p = 0.1893$; Monkey S, for 15° T1, $f(1,258) = 6.744$, $p = 0.0099$, LSD Fisher test: small CS, $p = 0.0035$, large CS, $p = 0.777$; for 30° T1; $f(1,244) = 4.647$, $p = 0.0321$, LSD Fisher test: small CS, $p = 0.0110$, large CS, $p = 0.5223$]. The increase in small CS latency caused by inactivation was significantly larger than that in PS latency, by about 20 ms for monkey S and monkey N ([inactivation trial CS latencies] − [mean control CS trial latency] vs. [inactivation trial PS latencies] − [mean control PS trial latency], unpaired *t* test (two-tailed); monkey N, $t(358) = 5.333$, $p < 1 \times 10^{-6}$; monkey S, $t(322) = 3.496$, $p < 1 \times 10^{-3}$).

To investigate whether ipsiversive and contraversive CSs are differentially impacted by LIP inactivation, we pooled the data from 15° and 30° PSs to increase statistical power. In both monkeys, inactivation increased the latency of contraversive as well as ipsiversive small CSs made after a PS to a contralesional target, indicating that the main factor associated with longer CS initiation latencies is the direction of the PS and not that of the CS [unpaired *t* test (two-tailed); Monkey N for small contraversive CS (control vs. inactivation), $t(62) = -2.8777$, $p = 0.0055$; small ipsiversive CS, $t(91) = -2.3912$, $p = 0.0188$; Monkey S for small contraversive CS, $t(39) = -2.0374$, $p = 0.0484$; small ipsiversive CS, $t(76) = -3.7287$, $p < 1 \times 10^{-3}$; Fig. 6, top panels]. In contrast, no effect was found for large CSs in either direction (Fig. 6, bottom panels).

Finally, examination of CSs made into the unimpaired visual hemifield show that LIP inactivation did not produce any significant effect on CS latency or accuracy following PSs to ipsilesional targets [unpaired *t* test (two-tailed), Table 4].

CS latency on no-jump trials follow the same pattern as target-jump trials.

To determine whether the pattern of latency impairments for small, but not large CS that we observed the context of CS induced by an intra-saccadic target displacement, is also present in naturally occurring CS following LIP inactivation, we analyzed the latency of CSs recorded during no-jump trials. This analysis is limited by the small number of CSs that could be recorded in this experimental condition. Pooling data from 15° and 30° T1 PS to increase statistical power, we found the same pattern as in target-jump

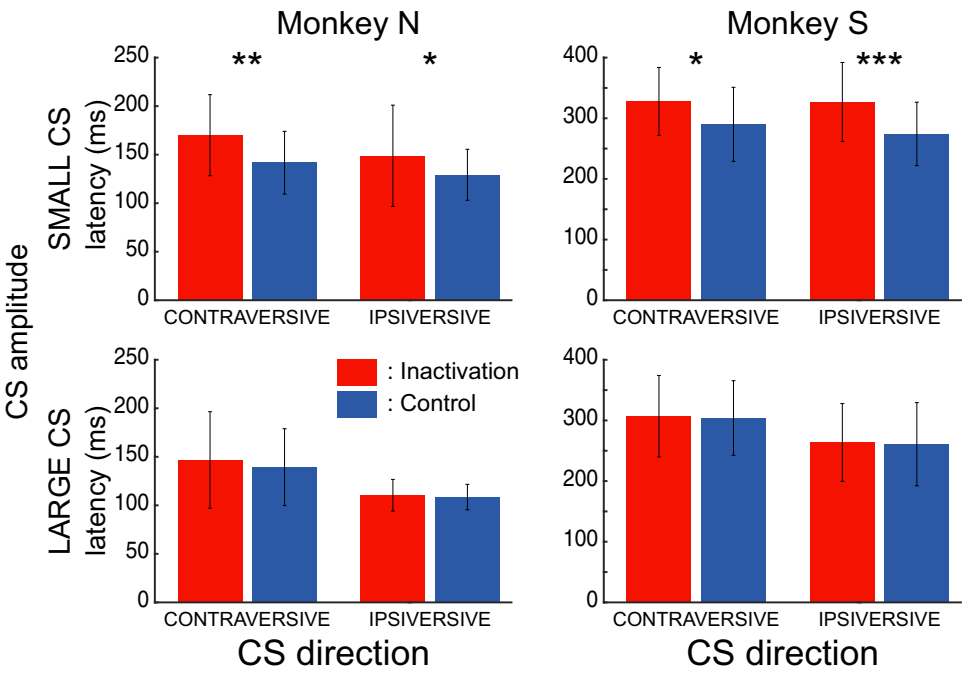

Fig. 6 Latency of small (top panels) and large (bottom panels) contraversive and ipsiversive corrective saccades (CS) in control vs. inactivation sessions performed after a primary saccade to the contralesional target (*$p < 0.05$; **$p < 0.01$; ***$p < 0.001$; error bars represent standard deviation)

Table 4 Results for CS in control vs. inactivation sessions after an ipsiversive PS

	Ipsiversive PS				
	Small CS		Large CS		
	Control	Inactivation	Control	Inactivation	
Latency	158 ± 50	155 ± 41	150 ± 37	156 ± 40	Monkey N
Accuracy	0.51 ± 0.53	0.57 ± 0.41	0.79 ± 0.67	0.67 ± 0.49	
Latency	335 ± 68	326 ± 62	298 ± 66	296 ± 66	Monkey S
Accuracy	1.02 ± 0.49	1.21 ± 0.6	1.27 ± 0.78	1.15 ± 0.59	

Latencies are represented in milliseconds and accuracies in degree (± for standard deviation)

trials with, in both monkeys, a 15 ms increase in the latency of small CS, compared to a 3 ms increase for large CS. This effect was significant in monkey N but not in monkey S, most likely because of the very small number of CS recorded in this animal [ANOVA, monkey N: small CSs 147 ms vs. 132 ms, large CSs 117 ms vs. 114 ms, for inactivation and control sessions, respectively; inactivation effect, $F(1,556) = 6.163$, $p = 0.0133$; small vs. large CS effect, $F(1,556) = 47.097$, $p < 1 \times 10^{-6}$, LSD fisher test, small CS (inactivation vs. control), $p = 0.0257$, large CS, $p = 0.2815$. Monkey S, small CSs 346 ms vs. 331 ms, large CSs 309 ms vs. 306 ms, for inactivation and control sessions, respectively; main effect $F(1,79) = 0.132$, $p = 0.7172$; inactivation effect, $F(1,79) = 0.264$, $p = 0.609$; small vs. large CS effect, $F(1,79) = 2.966$, $p = 0.089$, LSD Fisher test, small CS, $p = 0.3288$, large CS, $p = 0.9334$].

Comparison with primary saccades of the same amplitude as corrective saccades

Lastly, we tested whether the effect of LIP inactivation on small CS latency reflected a more general impairment for small saccades, independent of whether these are PSs or CSs. Indeed, it could be postulated that the effect on small CS could result from the injections centered into LIP sites dedicated to central visual field representation. To address such a possibility, our experimental protocol included a control condition in which monkeys executed visually guided saccades of small amplitude. These saccades were initiated from fixation points located at a horizontal eccentricity of 22.5° in the contralesional or ipsilesional field. Thus, this condition allowed us to select small PSs with orbital positions and metrics approximating closely those of the CSs made in the target-jump condition. We found only one significant effect of LIP inactivation on the small PSs [unpaired t test (two-tailed): $t(333) = -3.200$, $p = 0.0015$; trials with saccadic amplitude $\leq 3°$, Table 5]: monkey N showed slightly longer PS latencies for small contraversive saccades initiated from the contralesional field. Comparing Tables 5 and 6, this effect is smaller than all inactivation effects observed for CSs (e.g., 9 ms for small CS performed from contralesional field to the contralateral direction vs. 26 ms for CS performed from the contralesional field to the contra and ipsilateral direction, unpaired t test (two-tailed), $t(231) = -3.970$, $p < 1 \times 10^{-4}$) and more importantly happened in only one condition while the inactivation effect was present for the two monkeys in all saccadic directions. Thus, the effects of LIP inactivation on small PSs are smaller

Table 5 Results for small PS in control vs. inactivation sessions performed in the contralesional (A) and ipsilesional (B) field as a function of CS direction

A. Fixation point in the contralesional field

	CONTRAVERSIVE PS		IPSIVERSIVE PS		
	CONTROL	INACTIVATION	CONTROL	INACTIVATION	
Latency	208 ±26 **	217 ±24	207±18	207 ±21	Monkey N
	313±48	316±40	271 ±68	283 ±83	Monkey S

B. Fixation point in the ipsilesional field

	CONTRAVERSIVE PS		IPSIVERSIVE PS		
	CONTROL	INACTIVATION	CONTROL	INACTIVATION	
Latency	199 ±23	198 ±23	238±31	239 ±45	Monkey N
	280±88	278±66	342 ±104	347 ±102	Monkey S

Latencies are presented in milliseconds. Font types indicate significant differences (** for $p < 0.01$, ± for standard deviation)

Table 6 Summary of inactivation effect on saccade latency

	Monkey N				Monkey S			
	Contraversive PS		Ipsiversive PS		Contraversive PS		Ipsiversive PS	
Large PSs	**6.5**		4		**27**		0.5	
Small PS and CS								
Dir. Sacc	Contralateral	Ipsilateral	Contralateral	Ipsilateral	Contralateral	Ipsilateral	Contralateral	Ipsilateral
FP pos	Cont. field		Ips. field		Cont. field		Ips. field	
Small PS	**9**	0	−1	1	3	12	−2	5
Small CS	**28**	**20**	3	−8	**38**	**52**	−13	4

Entries in the table correspond to [inactivation latency] − [control latency] in milliseconds. Large positive values thus indicate a large increase in saccade latency. Value in bold face represent statistically significant differences between inactivation and control sessions

Dir. Sacc. direction of the saccade, *FP pos*. fixation point position, *Cont.* contralesional, *Ips.* ipsilesional

and less consistent across conditions compared to the effect on small CSs.

Discussion

Behavioral evidence from humans and monkeys suggests that to estimate and correct an imprecise saccadic eye movement, the oculomotor system relies on both a retinal error signal obtained from post-saccadic visual feedback as well as an extra-retinal error signal putatively obtained from efference copy and proprioception (Becker 1976; Munuera et al. 2009; Joiner et al. 2013). Retinal and extra-retinal sources of saccadic error have been shown to be optimally weighted during post-saccadic spatial updating (Munuera et al. 2009). Our single-neuron recording and inactivation results implicate area LIP in error processing related to contraversive PSs. A subpopulation of LIP neurons that fired only post-saccadically signaled a saccadic error by firing more strongly after an inaccurate PS. The cells' discharge did not depend on the execution of a CS or on the post-saccadic retinal feedback since the post-saccadic signal is equivalent whether or not a CS is executed to compensate the retinal post-saccadic error and the neurons are not responsive before the execution of small PSs towards peri-foveal visual targets. Our data constitute one of the few reports of a physiological correlate of an extra-retinal error signal in the brain. Zhou et al. (2016) also searched for saccadic error and correction signals in the posterior parietal cortex. They described visuomotor neurons which are active both before and after the primary saccade (named "pre- and post-saccadic response" (PPS) neurons). These cells showed a peri-saccadic burst of high rate activity encoding the intended PS vector, then about 250 ms after PS ending, a low-rate signal correlating with saccadic error and, importantly, CS execution probability. Thus, in contrast with this LIP subpopulation, the cells that we describe here exhibit post-saccadic but no visual and pre-saccadic activity and report the saccadic error, independent of whether a CS should be executed. We thus hypothesize that we identified a new and complementary class of parietal neurons involved in the detection of motor error that could integrate the early signals from the intended and executed saccade to compute the error signal that will be needed to generate a CS. This error signal, emerging approximatively 115 ms after the end of the PS, could then be relayed to the LIP subpopulation described in the Zhou et al.'s study which responds during PS execution and later predicts CS execution to correct the PS inaccuracy. Small extra-retinally signaled errors are known to improve visual exploration efficiency and to be useful for spatial updating after a saccade since the error amplitude after a first PS can be used to improve the accuracy of subsequent saccades in eye movement sequences even in the absence of visual feedback (Munuera et al. 2009). An error signal is also useful in driving saccadic adaptation (Wong and Shelhamer 2011a, b; 2012; Collins and Wallman 2012). Moreover, it is possible that studies in which subjects are rewarded for performing a saccade or a discrimination task on a target may lead to a weaker tolerance for saccadic error and a higher probability of CS execution since good oculomotor accuracy increases the chance of getting rewarded. Thus, this post-saccadic error mechanism could also be involved in signaling the distance to a reward, a process similar to previously observed reward-related mechanisms in LIP (Platt and Glimcher 1999; Kiani and Shadlen 2009). Thereby, the post-saccadic error signal we observe in LIP is potentially functional and could optimize many oculomotor-related behaviors, and not only corrective mechanisms.

The cerebellum, SC and FEF, three structures that are interconnected with LIP (Blatt et al. 1990; Paré and Wurtz 1997; Clower et al. 2001; Anderson et al. 2011), carry signals about an impeding saccade (Sommer and Wurtz 2002, 2006; Soetedjo et al. 2008a, b). We hypothesize that the spatially selective PS post-saccadic error signal in LIP that

we describe here could reflect a discrepancy between the retinotopic vector of the peripheral saccade target (≈ target − fixation point), a signal computed before the PS and observed many times in LIP (e.g., Andersen et al. 1992; Colby et al. 1996) and the signal associated to the saccade execution potentially generated by the SC or FEF. When this post-saccadic signal increases, signaling the detection of a motor error, other neurons, such as PPS neurons with CS-related activity (Zhou et al. 2016) and then neurons with peri-foveal visual RFs, would integrate (i.e., 'not ignore') the delayed post-saccadic visual signal of the target position (available only after its processing by visual areas). Thus, these neurons may contribute to the generation of a CS by coding the retinal error vector. Such neurons with peri-foveal RFs are known to exist in LIP (Ben Hamed et al. 2001; Ben Hamed and Duhamel 2002). Interestingly, a similar transfer of activity from LIP neurons with peripheral RFs to those with peri-foveal RFs to produce faster post-saccadic drifts of eye position has been proposed by another group (O'Leary and Lisberger 2012). Ultimately, this signal would be sent to a last neural ensemble (e.g., back to the SC, FEF or even the cerebellum) to plan a secondary (including corrective) saccade.

Importantly, our data also indicate a causal functional role for LIP in saccadic error processing. Indeed, reversibly inactivating LIP in one hemisphere by injecting muscimol caused small increases in the latency of initiation of PS, but even larger selective increases in the latency of small CSs. Inactivation effects on visually guided saccades is somewhat contentious, previous studies having reported mixed results with reports of presence (Li et al. 1999; Liu et al. 2010) or absence of impairment (Wardak et al. 2002) of contraversive saccade latencies. The reason for these inconsistent results across studies is unclear and may be due to differences in specific task conditions, in the quantity, concentration or injection speed of muscimol, or reflect individual variations of effects compounded by the small number of animals typically used in such studies. However, one result which is consistent with prior LIP inactivation studies is the preserved accuracy of all visually guided saccades, irrespective of the size or type (PS or CS).

The selective effects of muscimol on the latency of small CSs within the impaired hemifield were not error direction-dependent, since both contraversive and ipsiversive small CSs were affected. Similarly sized small PSs were not affected and neither were the small CSs following ipsiversive PSs. The critical condition associated with the CS latency increase is the prior execution of a PS in the contralesional direction. Interestingly, consistent with the present results, a report on patients with bilateral parietal cortex lesions and visuo-motor deficits (optic ataxia) showed delayed execution of CSs in a target-jump paradigm compared to control subjects (Gaveau et al. 2008). Our task did not distinguish between the role of PS direction (in the contraversive direction) or endpoint (in contralesional space) as the key element responsible for the delay in CS initiation, since all PSs were initiated from the center of the screen. Although both oculocentric and spatiotopic accounts could in principle explain our results, prior work suggests that the former is more likely as the main determinant of visually or memory-guided saccade impairments following LIP inactivation was found to be the direction of the saccade, irrespective of its starting position (Li and Andersen 2001).

Small vs. large CSs

In view of these findings, we speculatively suggest that the immediate post-saccadic period may represent a scenario where extra-retinal and retinal error information is combined, eventually leading to the execution of a CS. This scenario may only come into play for errors of small magnitude, likely to arise under natural circumstances as a result of moderate motor noise and target localization errors. In such a situation, LIP would play a role in evaluating whether a CS is needed, given the task at hand, i.e., whether the CS will improve the perception or needlessly slow down the exploration of a visual scene. Our data suggest that LIP is involved in this integration process and that the integration is lateralized to the hemifield where the PS is generated, thereby leading to an increase in saccade latency after LIP inactivation that is specific for small CSs following contraversive PSs, i.e., for CSs within the range of usual (and natural) saccadic error. In support of this hypothesis, evidence from cerebellar recordings indicate that complex spike discharges in the oculomotor vermis show a tuning for saccadic errors less than about 3°, suggesting a functional specialization for errors of this magnitude (Soetedjo et al. 2008a, b). Alternatively, the longer latency following inactivation may be due to potential re-engagement of fixation mechanisms. However, this is a less plausible explanation since the PS does not result in foveation of the saccade target. Furthermore, this interpretation cannot account for the lateralization of the deficit, which depends on the direction of the PS. Large CSs may involve a different process. As large saccadic errors likely result from poor saccade programming, the programming of corrective mechanisms might be made even before the retinal feedback is processed, making PS post-saccadic integration unnecessary. This hypothesis is supported by results from several previous studies showing that, in the absence of post-saccadic retinal feedback, i.e., when the target is extinguished during the execution of the PS, errors greater than 10% of the saccade amplitude lead almost systematically to a CS (Becker 1976; Ohl et al. 2013; Tian et al. 2013). These large corrections can be generated without engaging LIP post-saccadic processing.

Neurons discharging post-saccadically have been described in both the lateral convexity of the posterior parietal cortex (area 7a) and throughout the lateral bank of the intraparietal sulcus (area LIP), although it is considered that there is a higher proportion of such cells in the former than the latter region. (Barash et al. 1991a). Because of our a priori interest in post-saccadic neurons, we rapidly screened isolated units for such activity and we do not consider that the 38% of post-saccadic neurons in our data set reflects their actual prevalence in LIP. Also these post-saccadic neurons show a clear selectivity for saccades executed in the peripheral contralateral hemifield compare to saccades executed in the peripheral ipsilateral hemifield. To fully characterize these cell properties, future experiments should be performed to fully map their exact response fields in the contralateral field. However since these neurons increase their responses with the PS inaccuracy and because saccadic inaccuracy increases with movement amplitude, this would necessitate an extensive training of the monkeys to ensure that they would be able to perform large saccade with the same accuracy as that of the shorter ones. Nevertheless, the non-exhaustive mapping of the response fields does not rule out our statement that these cells encode an error signal related to the PS motor inaccuracy, since hypo- and hypermetric PSs (e.g., 13° vs. 17° PS eccentricity to T1 at 15°) carry the same pattern of neural discharge with a stronger post-saccadic response than accurate PSs (e.g., 15° PS).

We cannot also completely reject the possibility that some post-saccadic neurons recorded near the 7a/LIP border in the elbow of the IPS actually belong to this 7a. Similarly, since we had two depths of injections sites per track during the inactivation experiments (including one in the dorsal sector of LIP) and despite the fact that we left the cannulas in place during the sessions, we cannot rule out the possibility of some diffusion of injection bolus into the portion of area 7a closest to LIP. Furthermore, despite the fact that the stereotaxic recording coordinates were similar between the two animals, we cannot not completely reject the possibility that recordings in monkey S contain more 7a neurons that monkey N, since we did not perform histological verification on monkey S. Finally, the inactivation effects suggest that the more posterior and deeper subregion of LIP (LIPv) was consistently inactivated in both animals as significant effects were observed in both animals for large saccades, but it is not quite as clear for the more dorsal subregion (LIPd), since a significant increase in small (primary) saccade latencies was only observed in Monkey N.

Further experiments could also be performed to investigate whether the enhancement of the post-saccadic activity is related to the programming of saccade sequences, regardless of what triggers the second saccade (inaccurate first saccade or appearance of a novel target). However, it is unlikely that the post-saccadic modulation is linked to the programming of a saccadic sequence. Indeed, the LIP post-saccadic response is lower for accurate than inaccurate PSs in the target-jump condition even though in both cases the monkeys perform a sequence of two saccades to reach the displaced target position in the target-jump condition, a strong argument that having to execute an unexpected second saccade cannot account for the observation neuronal activity modulation.

Our conclusions can only be viewed as tentative at this point. We provide evidences about a role of the parietal cortex in oculomotor corrective mechanisms but we did not disentangle whether LIP is only involved in the intention to perform a correction or only in the attentional mechanisms leading to the detection of the error. Therefore, further experiments, including investigation in area 7a, will be needed to resolve these questions. Nevertheless, our two complementary experiments suggest that the posterior parietal cortex is part of an oculomotor performance monitoring system relying on internal and external feedback loops and that it plays critical roles in reporting saccadic error and in the computational steps leading up to the recruitment of corrective mechanisms aimed at adjusting eye position on the saccade target.

Acknowledgements The authors of this article are grateful to Leon Tremblay for his valuable advice during inactivation experiments, Suresh B. Krishna for reading and commenting this manuscript and Sandra Duperrier for histological analysis.

Funding This work was supported by the LABEX (ANR-11—LABEX-0042) of University de Lyon within the program "Investissement d'Avenir", and by Agence Nationale de la Recherche (ANR-06-NEURO-024-01) to J-R.D. and by the Fondation pour la Recherche Médicale for J.M. (FDT20070910790).

Compliance with ethical standards

Conflicts of interest The authors declare no competing financial interests.

References

Andersen RA, Brotchie PR, Mazzoni P (1992) Evidence for the lateral intraparietal area as the parietal eye field. Curr Opin Neurobiol 2:840–846. https://doi.org/10.1016/0959-4388(92)90143-9

Anderson JC, Kennedy H, Martin KAC (2011) Pathways of attention: synaptic relationships of frontal eye field to V4, lateral intraparietal cortex, and area 46 in macaque monkey. J Neurosci 31:10872–10881. https://doi.org/10.1523/JNEUROSCI.0622-11.2011

Barash S, Bracewell RM, Fogassi L et al (1991a) Saccade-related activity in the lateral intraparietal area: I. Temporal properties; comparison with area 7a. J Neurophysiol 66:1095–1108

Barash S, Martyn R, Andersen A (1991b) Saccade-related activity in the lateral intraparietal area II. Spatial properties. J Neurophysiol 66:1109–1124

Becker W (1972) The control of eye movements in the saccadic system. Bibl Ophthalmol Suppl ad Ophthalmol 82:233–243

Becker W (1976) Do correction saccades depend exclusively on retinal feedback? A note on the possible role of non-retinal feedback. Vision Res 16:425–427. https://doi.org/10.1016/0042-6989(76)90209-1

Becker W (1991) Saccades. In: Carpenter R (ed) Eye movements. MacMillan, London, pp 95–137

Ben Hamed S, Duhamel JR (2002) Ocular fixation and visual activity in the monkey lateral intraparietal area. Exp Brain Res 142:512–528. https://doi.org/10.1007/s00221-001-0954-z

Ben Hamed S, Duhamel J-RR, Bremmer F et al (2001) Representation of the visual field in the lateral intraparietal area of macaque monkeys: a quantitative receptive field analysis. Exp Brain Res 140:127–144. https://doi.org/10.1007/s002210100785

Bergeron A, Matsuo S, Guitton D (2003) Superior colliculus encodes distance to target, not saccade amplitude, in multi-step gaze shifts. Nat Neurosci 6:404–413. https://doi.org/10.1038/nn1027

Blatt GJ, Andersen RA, Stoner GR (1990) Visual receptive field organization and cortico-cortical connections of the lateral intraparietal area (area LIP) in the macaque. J Comp Neurol 299:421–445. https://doi.org/10.1002/cne.902990404

Bridgeman B, Hendry D, Stark L (1975) Failure to detect displacement of the visual world during saccadic eye movements. Vision Res 15:719–722. https://doi.org/10.1016/0042-6989(75)90290-4

Clower DM, West RA, Lynch JC, Strick PL (2001) The inferior parietal lobule is the target of output from the superior colliculus, hippocampus, and cerebellum. J Neurosci 21:6283–6291

Colby CL, Duhamel JR, Goldberg ME (1996) Visual, presaccadic, and cognitive activation of single neurons in monkey lateral intraparietal area. J Neurophysiol 76:2841–2852. https://doi.org/10.1152/jn.1996.76.5.2841

Collins T, Wallman J (2012) The relative importance of retinal error and prediction in saccadic adaptation. J Neurophysiol 107:3342–3348. https://doi.org/10.1152/jn.00746.2011

Daniel PM, Whitteridge D (1961) The representation of the visual fiel on the cerebral cortex in monkeys. J Physiol 159:203–221

Deubel H, Wolf W, Hauske G (1982) Corrective saccades: effect of shifting the saccade goal. Vision Res 22:353–364. https://doi.org/10.1016/0042-6989(82)90151-1

Duhamel J-R, Colby CL, Goldberg ME (1992) The updating of the representation of visual space in parietal cortex by intended eye movements. Science 255:90–92

Gaveau V, Pélisson D, Blangero A et al (2008) Saccade control and eye-hand coordination in optic ataxia. Neuropsychologia 46:475–486. https://doi.org/10.1016/j.neuropsychologia.2007.08.028

Gnadt JW, Andersen RA (1988) Memory related motor planning activity in posterior parietal cortex of monkey. Exp Brain Res 70:216–220

Goffart L, Chen LL, Sparks DL (2004) Deficits in saccades and fixation during muscimol inactivation of the caudal fastigial nucleus in the rhesus monkey. J Neurophysiol 92:3351–3367. https://doi.org/10.1152/jn.01199.2003

Gottlieb JP, Kusunoki M, Goldberg ME (1998) The representation of visual salience in monkey parietal cortex. Nature 391:481–484. https://doi.org/10.1038/35135

Hays AV, Richmond BJ, Optican LM (1982) A UNIX-based multiple process system for real-time data acquisition and control. WESCON Conf Proc 2:1–10

Horan M, Daddaoua N, Gottlieb J (2019) Parietal neurons encode information sampling based on decision uncertainty. Nat Neurosci. https://doi.org/10.1038/s41593-019-0440-1

Huk AC, Katz LN, Yates JL (2017) The role of the lateral intraparietal area in (the study of) decision making. Annu Rev Neurosci 40:349–372. https://doi.org/10.1146/annurev-neuro-072116-031508

Joiner WM, Fitzgibbon EJ, Wurtz RH (2010) Amplitudes and directions of individual saccades can be adjusted by corollary discharge. J Vis 10:1–12. https://doi.org/10.1167/10.2.22.Introduction

Joiner WM, Cavanaugh J, FitzGibbon EJ, Wurtz RH (2013) Corollary discharge contributes to perceived eye location in monkeys. J Neurophysiol 110:2402–2413. https://doi.org/10.1152/jn.00362.2013

Judge SJ, Richmond BJ, Chu FC (1980) Implantation of magnetic search coils for measurement of eye position: an improved method. Vis Res 20:535–538

Kiani R, Shadlen MN (2009) Representation of confidence associated with a decision by neurons in the parietal cortex. Science. https://doi.org/10.1126/science.1169405

Li CR, Andersen RA (2001) Inactivation of macaque lateral intraparietal area delays initiation of the second saccade predominantly from contralesional eye positions in a double-saccade task. Exp Brain Res. https://doi.org/10.1007/s002210000546

Li CS, Mazzoni P, Andersen RA (1999) Effect of reversible inactivation of macaque lateral intraparietal area on visual and memory saccades. J Neurophysiol 81:1827–1838. https://doi.org/10.1152/jn.1999.81.4.1827

Liu Y, Yttri EA, Snyder LH (2010) Intention and attention: different functional roles for LIPd and LIPv. Nat Neurosci 13:495–500. https://doi.org/10.1038/nn.2496

Morel P, Deneve S, Baraduc P (2011) Optimal and suboptimal use of postsaccadic vision in sequences of saccades. J Neurosci 31:10039–10049. https://doi.org/10.1523/JNEUROSCI.0492-11.2011

Munuera J, Morel P, Duhamel J-R, Deneve S (2009) Optimal sensorimotor control in eye movement sequences. J Neurosci. https://doi.org/10.1523/JNEUROSCI.1169-08.2009

O'Leary JG, Lisberger SG (2012) Role of the lateral intraparietal area in modulation of the strength of sensory-motor transmission for visually guided movements. J Neurosci 32:9745–9754. https://doi.org/10.1523/JNEUROSCI.0269-12.2012

Ohl S, Brandt SA, Kliegl R (2013) The generation of secondary saccades without postsaccadic visual feedback. J Vis 13:11–11. https://doi.org/10.1167/13.5.11

Panouillères M, Alahyane N, Urquizar C et al (2013) Effects of structural and functional cerebellar lesions on sensorimotor adaptation of saccades. Exp Brain Res 231:1–11. https://doi.org/10.1007/s00221-013-3662-6

Paré M, Wurtz RH (1997) Monkey posterior parietal cortex neurons antidromically activated from superior colliculus. J Neurophysiol 78:3493–3497. https://doi.org/10.1152/jn.1997.78.6.3493

Platt ML, Glimcher PW (1999) Neural correlates of decision variables in parietal cortex. Nature 400:233–238

Popa LS, Streng ML, Hewitt AL, Ebner TJ (2016) The errors of our ways: understanding error representations in cerebellar-dependent motor learning. Cerebellum 15:93–103

Prablanc C, Jeannerod M (1975) Corrective saccades: dependence on retinal reafferent signals. Vision Res 15:465–469. https://doi.org/10.1016/0042-6989(75)90022-X

Rayner K (1998) Eye movements in reading and information processing. Psychol Bull 124:372–422. https://doi.org/10.1080/13803395.2011.639298

Robinson FR, Fuchs AF (2001) The role of the cerebellum in voluntary eye movements. Annu Rev Neurosci 24:981–1004. https://doi.org/10.1146/annurev.neuro.24.1.981

Shadmehr R, Smith MA, Krakauer JW (2010) Error correction, sensory prediction, and adaptation in motor control. Annu Rev Neurosci 33:89–108. https://doi.org/10.1146/annurev-neuro-060909-153135

Soetedjo R, Fuchs AF (2006) Complex spike activity of purkinje cells in the oculomotor vermis during behavioral adaptation of monkey saccades. J Neurosci 26:7741–7755. https://doi.org/10.1523/JNEUROSCI.4658-05.2006

Soetedjo R, Kojima Y, Fuchs A (2008a) Complex spike activity signals the direction and size of dysmetric saccade errors. Prog Brain Res 171:153–159

Soetedjo R, Kojima Y, Fuchs AF (2008b) Complex spike activity in the oculomotor vermis of the cerebellum: a vectorial error signal for saccade motor learning? J Neurophysiol 100:1949–1966. https://doi.org/10.1152/jn.90526.2008

Sommer MA, Wurtz RH (2002) A pathway in primate brain for internal monitoring of movements. Science 296:1480–1482. https://doi.org/10.1126/science.1069590

Sommer MA, Wurtz RH (2006) Influence of the thalamus on spatial visual processing in frontal cortex. Nature. https://doi.org/10.1038/nature05279

Sommer MA, Wurtz RH (2008) Brain circuits for the internal monitoring of movements. Annu Rev Neurosci 31:317–338. https://doi.org/10.1146/annurev.neuro.31.060407.125627

Thiele A, Henning P, Kubischik M, Hoffmann KP (2002) Neural mechanisms of saccadic suppression. Science 295:2460–2462. https://doi.org/10.1126/science.1068788

Thier P, Dicke PW, Haas R et al (2002) The role of the oculomotor vermis in the control of saccadic eye movements. Ann NY Acad Sci 978:50–62

Tian J, Ying HS, Zee DS (2013) Revisiting corrective saccades: role of visual feedback. Vision Res 89:54–64. https://doi.org/10.1016/j.visres.2013.07.012

van Beers RJ (2007) The sources of variability in saccadic eye movements. J Neurosci 27:8757–8770. https://doi.org/10.1523/JNEUROSCI.2311-07.2007

van Beers RJ (2008) Saccadic eye movements minimize the consequences of motor noise. PLoS ONE. https://doi.org/10.1371/journal.pone.0002070

van Beers RJ, Haggard P, Wolpert DM et al (2004) The role of execution noise in movement variability. J Neurophysiol 91:1050–1063

Waitzman DM, Ma TP, Optican LM, Wurtz RH (1988) Superior colliculus neurons provide the saccadic motor error signal. Exp Brain Res 72:649–652. https://doi.org/10.1007/BF00250610

Wang X, Zhang M, Cohen IS, Goldberg ME (2007) The proprioceptive representation of eye position in monkey primary somatosensory cortex. Nat Neurosci. https://doi.org/10.1038/nn1878

Wardak C, Olivier E, Duhamel J-R (2002) Saccadic target selection deficits after lateral intraparietal area inactivation in monkeys. J Neurosci 22:9877–9884

Wardak C, Olivier E, Duhamel JR (2004) A Deficit in covert attention after parietal cortex inactivation in the monkey. Neuron 42:501–508. https://doi.org/10.1016/S0896-6273(04)00185-0

Weber RB, Daroff RB (1972) Corrective movements following refixation saccades: type and control system analysis. Vision Res 12:467–475. https://doi.org/10.1016/0042-6989(72)90090-9

Wong AL, Shelhamer M (2011a) Sensorimotor adaptation error signals are derived from realistic predictions of movement outcomes. J Neurophysiol 105:1130–1140. https://doi.org/10.1152/jn.00394.2010

Wong AL, Shelhamer M (2011b) Exploring the fundamental dynamics of error-based motor learning using a stationary predictive-saccade task. PLoS ONE. https://doi.org/10.1371/journal.pone.0025225

Wong AL, Shelhamer M (2012) Using prediction errors to drive saccade adaptation: the implicit double-step task. Exp Brain Res 222:55–64. https://doi.org/10.1007/s00221-012-3195-4

Zhou Y, Liu Y, Lu H et al (2016) Neuronal representation of saccadic error in macaque posterior parietal cortex (PPC). Elife. https://doi.org/10.7554/eLife.10912